Design of Solar Field and Performance Estimation of Solar Tower Plants

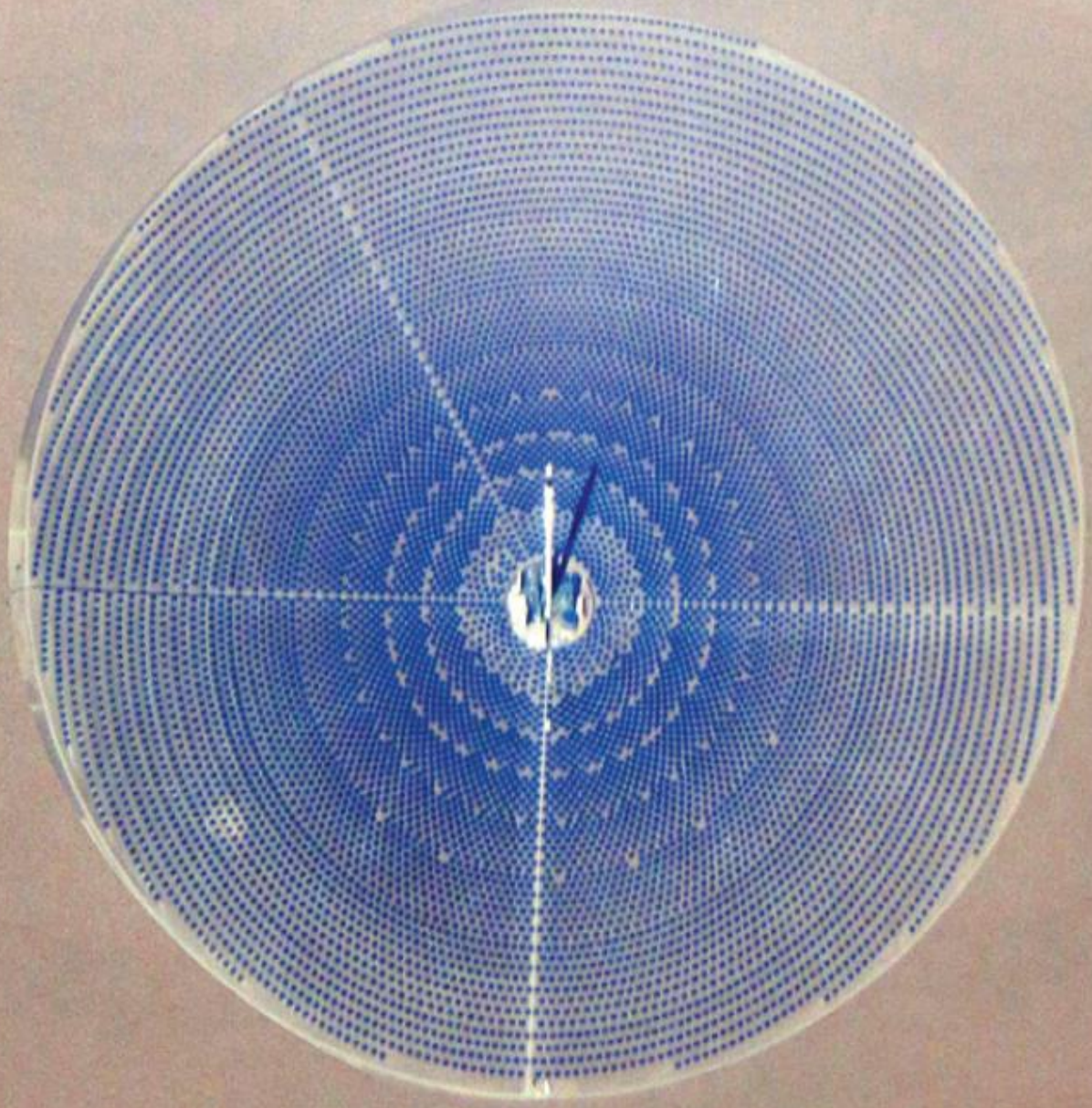

May 2016

CSTEP
CENTER FOR STUDY OF SCIENCE, TECHNOLOGY & POLICY

SERIIUS

Design of Solar Field and Performance Estimation of Solar Tower Plants

Authors

G Srilakshmi

M A Ramaswamy

Thirumalai N C

May 2016

Center for Study of Science, Technology and Policy (CSTEP) is a private, not-for-profit (Section 25) Research Corporation registered in 2005.

Designing and Editing by CSTEP

(CSTEP-Report-2016-06)

May, 2016

Center for Study of Science, Technology and Policy

18, 10th Cross, Mayura Street,

Papanna Layout, Nagashettyhalli, RMV II Stage,

Bangalore-560094 Karnataka, INDIA

Tel.: +91 (80) 6690-2500

Fax: +91 (80) 2351-4269

Email: cpe@cstep.in

Website: www.cstep.in

Acknowledgement

The support and encouragement given by Dr. V. S. Arunachalam, Chairman, CSTEP and Dr. Anshu Bharadwaj, Executive Director, CSTEP is deeply appreciated. We would also like to thank Dr. Mridula Dixit Bharadwaj, Principal Research Scientist, CSTEP for her continuous support and guidance. We are thankful to Suresh N S, Sr. Research Engineer and Badri S Rao, Sr. Research Engineer, CSTEP for their critical review and comments in improving the document. We are also thankful to Chaitanya Kanth, Sr. Research Engineer and Smita K Dolly, Sr. Research Engineer, CSTEP for their help in developing a user interface tool for analysis. We also thank the Communication and Policy Engagement team for their support.

This work is supported in part under the US-India Partnership to Advance Clean Energy-Research (PACE-R) for the Solar Energy Research Institute for India and the United States (SERIIUS), funded jointly by the U.S. Department of Energy (Office of Science, Office of Basic Energy Sciences, and Energy Efficiency and Renewable Energy, Solar Energy Technology Program, under Subcontract DE-AC36-08GO28308 to the National Renewable Energy Laboratory, Golden, Colorado) and the Government of India, through the Department of Science and Technology under Subcontract IUSSTF/JCERDC-SERIIUS/2012 dated 22nd November, 2012

Contents

Nomenclature

Symbol	Variable Name	Units
A	Azimuth angle	$Degrees$
A^1	Intermediate azimuth angle	$Degrees$
CUF	Capacity Utilisation factor	
DNI_{annual}	Annual solar resource	Wh/m^2
DNI_i	Hourly Direct Normal Irradiance at the location for the i^{th} hour	W/m^2
E_{tea}	Thermal energy available from storage	Wh
$E_{tes,max}$	Maximum amount of thermal energy that can be stored	Wh
LA	Total land area	m^2
LA_n	Total land area of n^{th} row	m^2
L_f	Loss factor	
MA	Total mirror area	m^2
MA_n	Total mirror area of n^{th} row	m^2
N_f	Number of points under boundary chosen by user	
PD	Packing density at point p of the field	
$P_{cap,d}$	Design plant capacity	MW
$P_{i,a}$	Power per unit land area of field	W
P_{amax}	Maximum of $P_{i,a}$ values	W
$P_{g,d}$	Rated gross power	W

$P_{htf,d}$	Thermal power input to the heat exchanger at design	W
$P_{htf,i}$	Thermal power input to the heat exchanger from solar field for the i^{th} hour	W
P_i	Power to heat exchanger divided by the square of the height of the tower, due to all points j for each hour i	W
P_{imax}	Maximum of all P_i values	W
P_{max}	Maximum of the P_i values (over 8760 hours)	W
$P_{s,d}$	Design solar power required from the field	W
SM	Solar Multiple	
$S_{n,j}$	Slant distance from point j of the solar field to receiver (this is effectively $S_{n,nd,j} \times h$)	km
$S_{n,nd,j}$	Non-dimensional slant height of point j	km/m
$\frac{d_x}{h}$ and $\frac{d_y}{h}$	Non-dimensional length/width of elemental area	
e_g	Gross electrical energy that would be generated during the hour without considering energy needed for start-up	Wh
e_{ga}	Gross hourly electrical energy available after accounting for start-up	Wh
$e_{ga,t}$	Total annual gross electrical energy available	Wh
e_{grid}	Electrical energy supplied to grid	Wh
$e_{grid,t}$	Total annual gross electrical energy supplied to the grid	Wh
e_{hb}	Electrical energy apportioned to hybridisation	Wh

$e_{hb,t}$	Total annual gross electrical energy apportioned to hybridisation	Wh
e_l	Annual reflected energy per unit land area of the solar field (taking into account cosine effect and packing density)	Wh/m^2
$e_{lchosen}$	Value of e_l contour chosen by user	
e_m	Annual reflected energy per unit mirror area of field (taking into account only cosine effect)	Wh/m^2
e_s	Hourly electrical energy apportioned to solar input	Wh
$e_{s,t}$	Total annual gross electrical energy apportioned to solar input	Wh
e_{start}	Equivalent electrical energy required for start-up accounting for thermal losses during shut down period	Wh
f_{hb}	Fraction of hybridisation power	
$f_{hb,t}$	Total annual fraction of hybridisation used	
$f_{hb,used}$	Actual hybridisation fraction used	
f_p	Fraction of the gross electrical power generated ignoring thermal losses during shutdown	
f_{pa}	Ratio of electrical power generated to the rated capacity	
f_{th}	Fraction of thermal power delivered to power block	
$f_{th,d}$	This is the design fraction of energy with the HTF. Its value is = 1.	
$f_{th,m}$	Modified fraction of thermal power $(f_{th} + f_{th,sta})$	

$f_{th,max}$	Maximum fraction of thermal power permitted	
$f_{th,min}$	Minimum fraction of thermal power required for power generation	
$f_{th,s}$	Solar thermal power as a fraction of the design thermal power	
$f_{th,st}$	Fraction of thermal power used from storage	
$f_{th,sta}$	Fraction of thermal power available from storage	
$f_{th,T}$	Total fraction of thermal power $(f_{th,m} + f_{hb})$	
h	Height of the tower	m
$h[1]$	Final height of tower at $SM = 1$	m
$h[SM]$	Height of tower for given SM	m
$h_{new}[1]$	New height calculated based on iteration	m
i	Number of the hour (varies from 1 to 8760)	
j	Set of all points under boundary (varies from 1 to N_f)	
n	Day of year (varies from 1 to 365)	
n_n	Number of heliostats in n^{th} row	
p	Each point in the field	
r	Radial distance from base of tower to point in field	m
r_{n-1}	Radial distance from base of tower to the $(n-1)^{th}$ row of heliostats	m
r_n	Radial distance from base of tower to the n^{th} row of heliostats	m

r_{n+1}	Radial distance from base of tower to the $(n+1)^{th}$ row of heliostats	m
r/h	Non-dimensionalised radial distance of point $(x/h, y/h)$ from the tower	
$\left(\frac{r}{h}\right)_{min}$	Minimum non-dimensional distance of solar field from tower	
t	Hour of day (varies from 0 to 24)	
t_s	Number of hours of thermal storage	$Hours$
$t_{shutdown}$	Hours for which plant is shut down	$Hours$
x/h	Non-dimensionalised x coordinate of point on field	
y/h	Non-dimensionalised y coordinate of point on field	
α	Altitude angle	$Degrees$
δ	Solar declination angle	$Degrees$
Δh	Height increment	m
Δt	Time step	$hours$
$\Delta\theta$	Angle subtended by farthest two heliostats of a row	$radians$
$\Delta\emptyset$	Circumferential angle between heliostat centres	$radians$
$\eta_{actual,pb}$	Actual power block efficiency	$as\ fraction$
$\eta_{att,j}$	Attenuation efficiency of point j	$as\ fraction$
$\eta_{gross-max}$	Maximum power block efficiency	$as\ fraction$
η_{he}	Heat exchanger efficiency	$as\ fraction$

η_m	Mirror efficiency	$as\ fraction$
η_{pb}	Power block efficiency	$as\ fraction$
$\eta_{receiver}$	Receiver efficiency	$as\ fraction$
$\eta_{rel,pb}$	Ratio of actual and maximum gross power block efficiency	$as\ fraction$
η_{s-e}	Annual solar to electric conversion efficiency	$in\ \%$
η_{st}	Thermal storage efficiency	$as\ fraction$
ϕ	Latitude of the location	$Degrees$
θ_i	Cosine angle for hour i	$Degrees$
$\theta_{i,p}$	Angle of incidence of Sun ray for hour i and point p	$Degrees$
$\theta_{i,j}$	Angle of incidence of Sun ray for hour i and point j	$Degrees$
θ_Z	Zenith angle	$Degrees$
ω	Solar hour angle	$Degrees$

List of Figures

List of Tables

1. Introduction

Solar Tower (ST) makes use of a large number of heliostats or mirrors (which have a dual axis control system in order to track the sun's rays throughout the day) to reflect solar energy impinging on them onto a receiver which is located at the top of a tower. The concentrated solar energy that falls on the receiver is transferred to a Heat Transfer Fluid (HTF) which passes through the receiver. The thermal energy of HTF is then transferred to a working fluid in the power block, by means of a heat exchanger, thereby generating electricity. ST systems generally have a storage component which allows for a part of the solar energy that is collected, to be stored for later use (during night time/peak demand periods).

The major components in a ST plant are the heliostats, receivers, tower, HTF, working fluid and power block. A description of these variants as well as an assessment of the existing ST plants worldwide is available in a report titled – "Global Review of Solar Tower Technology" (Srilakshmi, Venkatesh, Badri, Thirumalai, & Ramaswamy, 2014).

The available literature on ST covers component level analyses (specifically on heliostats and their tracking mechanisms), shadowing and blocking effect algorithms, receiver heat transfer analyses, heliostat layout optimisation studies etc. However, the present literature lacks a systematic, overall methodology to model a complete ST plant from scratch (with given inputs such as plant capacity, location, gross efficiencies etc.).

The primary objective of this study is to develop a methodology to carry out a technical analysis of an ST, similar to the one carried out for a Parabolic Trough (PT) in CSTEP's Solar Techno-Economic Model (CSTEM). The working model of the PT tool is described in detail in a CSTEP report titled 'Engineering Economic Policy Assessment of Concentrating Solar Thermal Power Technologies for India' (MA Ramaswamy V. C., 2012). While attempting to do this, it was realised that there were so many fundamental differences between PT and ST technologies, that a straightforward extension of the methodology could not be used for ST. Section 2 addresses the details of these differences.

By studying these differences, it becomes clear that the crux of the issue is that in the case of PT, solar energy that can be collected by the receiver is directly proportional to the land area of the solar field. However, in the case of ST, solar energy that can be collected by the solar field is a complex function of the solar field layout, relative to the tower. From existing literature, no leads or suggestions are available as to how to decide the tower height or fix the boundary of the solar field with respect to the tower. Therefore, the first pre-requisite for developing the methodology was to obtain a rational method for fixing the boundary of the solar field around the tower in terms of variation of non-dimensional quantity r/h, with respect to the azimuth angle (where r is the radial distance from the tower and h is the height of the tower). Without arriving at this coupling between the solar field boundary and the tower height in non-dimensional terms, it would not have been possible to arrive at a methodology analogous to that developed for PT. Section 3 deals with the method of defining the solar field boundary.

The scope of this study is restricted to arrive at a rational approach to determine the optimum solar field and the associated tower height for an ST using an external cylindrical receiver, using molten salt as both HTF and storage medium operating with steam Rankine power cycle. In the case of a cavity receiver, the field is also intimately coupled with the design of the cavity

receiver (the angle subtended by the opening of the receiver etc.). The angle subtended by the field is a function of the type of cavity and is not very amenable for generalisation. However, if this angle is known, the present study can be extended for cavity receivers as well.

Section 4 gives an overview of the methodology and Section 5 describes the methodology in detail.

A case study on hypothetical ST plants located at Jodhpur, for various capacities, with different hybridisation and thermal storage capacities is presented in Section 6. In this study, the solar field for Solar Multiple (SM) equal to 1 and the optimum values of SM for various cases with the consideration of maximum annual solar to electric conversion efficiency are presented.

This study will be extended later on to get optimum values of SM based on LCOE (similar to CSTEM for PT) after a study of the cost of various components and financial parameters associated with ST technology is undertaken.

In order to maintain a smooth flow of thought in the main text, details that have gone into the determination of the nominal Packing Density (PD) variation with r/h and choice of the solar field boundary are explained in Appendix 1 and Appendix 2. Appendix 3 gives the flowchart that was used in the coding of this methodology for the CSTEM tool. The programming language used for writing the code for this methodology is JAVA.

2. Fundamental Differences between PT and ST Technology

As mentioned, there are some fundamental differences between PT and ST technology because of which the methodology that was developed for PT (used in CSTEM), cannot be directly extended for ST. These differences are explained in detail in this section.

2.1. Overview

i. In an ST plant, the solar power captured is not proportional to the solar field unlike for a PT plant.
ii. In case of ST, the solar energy received by each heliostat is different (depending on its location from the tower) as the cosine effect is different for different heliostats, unlike that for PT where the cosine effects are same for all troughs.
iii. PD which is a ratio of the mirror area to land area, is different for different locations in the ST field to minimise the shadowing and blocking effects.
iv. The receiver is an integral part of the PT system whereas for the ST system, single or multiple receivers (at the top of the tower) are used for all the heliostats. Therefore, the height of the tower also plays a major role. The type of receiver may vary in case of tower (cavity, external cylindrical, volumetric etc.). The choice of receiver type also depends on the power cycle used. There are many such interdependencies to be taken into account while modelling an ST plant.
v. The effect of attenuation can be neglected in the case of PT, whereas, it has to be taken into account for an ST plant. This is because heliostats can be located at a distance of 1 km from the tower. A reflected ray travelling through the atmosphere for such long distances is bound to undergo significant amounts of absorption and scattering, thereby, decreasing the energy impinging on the receiver.

2.2. Packing Density

In the case of PT, PD is uniform throughout the field and its value is fairly well established.

On the contrary, in the case of ST, to minimise blocking effects, radial spacing of heliostats increases as the ratio r/h increases, where $'r'$ is the radial distance of a heliostat from the tower and $'h'$ is the tower height. The circumferential spacing of heliostats is generally governed by the staggered field pattern used. Here, the gap between the radial locations of two adjacent heliostats is approximately equal to the heliostat width for the first row. Subsequent rows with increasing r/h are arranged in a staggered manner. Overall, PD decreases as r/h increases. The manner in which PD varies with r/h is also not explicitly given in open literature. From the information, available for various existing ST plants, a nominal variation for PD with r/h has been arrived at (refer to Appendix 1).

2.3. Relation between Solar Energy Collected and Solar Field

Solar energy that is collected by the mirrors and directed towards the receiver is directly proportional to the size of the solar field in case of the PT, whereas, for ST, it is a complex function of the solar field layout, pattern of heliostats used in the field and height of the tower.

In the case of PT, if one wishes to double the solar energy collected by the receiver, then one has to double the solar field area as well. On the other hand, in the case of an ST, there is no clarity in literature available as to how to go about it. Does one keep the same tower height and increase the solar field? Or does one have to simultaneously increase tower height and solar field area, in which case, what is the rational approach to increase both of them? These are some of the relevant questions that need to be answered in order to develop any modelling methodology for this technology.

Due to the coupling between the solar field size and tower height, no logical approach has been indicated in open literature to arrive at the solar field area and tower height. For all existing ST plants, no information is available on the methodology used to arrive at that solar field and tower height. They are probably trade secrets.

2.4. Tower Height

Though the height of the tower is a critical parameter, a specific method to arrive at the tower height is not available. It can be seen that a plot of the tower height vs. capacity of existing plants shows no definite trend (Figure 1).

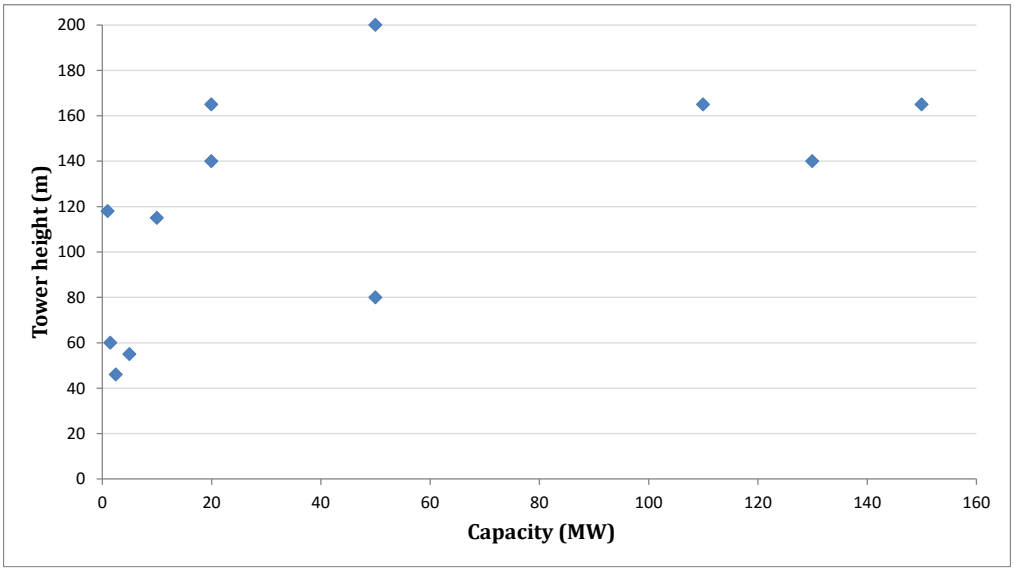

Figure 1: Tower Height Variation with Capacity of Existing Plants

One may expect that if thermal storage is provided then a greater height might be needed for the same capacity. So, a term called equivalent capacity was introduced to take into account the storage component of Concentrated Solar Power (CSP) plants assuming that a normal plant would operate for 9 hours a day. It is calculated as follows:

$$Equivalent\ Capacity = Rated\ Capacity \times \left(\frac{9+x}{9}\right) \qquad (1)$$

where x is the number of hours of thermal storage that the plant provides.

Even when the height is plotted vs. equivalent capacity, there is no definite trend (see Figure 2; (Srilakshmi, Venkatesh, Badri, Thirumalai, & Ramaswamy, 2014).

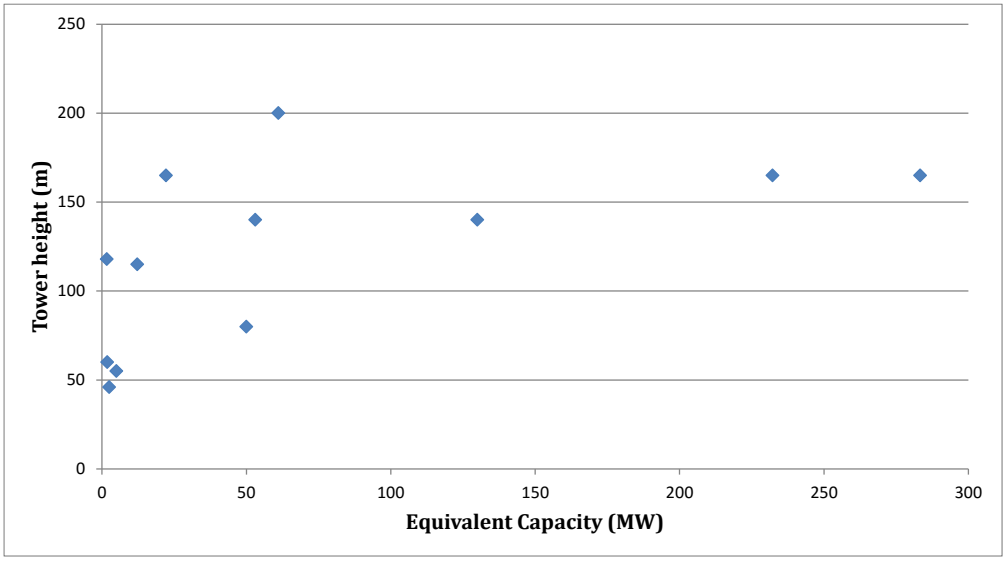

Figure 2: Tower Height Variation with Equivalent Capacity

2.5. Solar Field Boundary Relative to the Tower

In the case of PT, the solar field is uniform everywhere, but for ST, the optimum solar field is intimately coupled to the tower height, the latitude of the plants location and also the type of receiver and field layout used. If one examines solar fields that have been used in existing CSP plants with ST technology, it can be observed that there is a lot of variation depending on whether a cavity receiver or an external cylindrical receiver has been used.

The present study is limited to solar field of ST plants using external cylindrical receiver (where there seems to be some general pattern). From a review conducted on the existing ST plants, out of about 615 MW (the total installed capacity worldwide), more than about 90% of these plants have a surround field with a radial staggered configuration (Srilakshmi, Venkatesh, Badri, Thirumalai, & Ramaswamy, 2014). Therefore, developing a method for this type of solar field was considered to be most relevant.

In these types of solar fields, mirrors are located along a circular arc at various radii from the tower which are defined as rows. Mirrors in rows are kept at staggered azimuth angles. For the Gemasolar plant (see Figure 3 – Source: http://wikimapia.org/#lang=en&lat=37.564548&lon=-5.326610&z=15&m=b) which is located at a latitude of about 37°N, the solar field is approximately circular, but the tower is not at the centre of this circular field. It is slightly to the south of the centre for ST plants located in the northern hemisphere. This can also be seen in Figure 3.

Figure 3: Gemasolar ST Plant in Spain

In other words, with respect to the tower, the field extends more towards the north than to the south. However, no guidelines are available as to how the variation of the radial distance of heliostats with respect to azimuth is determined. If the useful annual solar energy that can be collected by a mirror of unit area is considered for a plant located in the higher northern

latitudes, energy from all mirrors located to the north of the tower is far superior to what is obtained from a heliostat located to the south of it.

If the solar field boundary were to be fixed on the basis of a contour around the tower yielding some energy value per unit mirror area, then that contour (as shown in Section 3.2) will be much more oblong than what has been used in the existing plants. That is, the radial distance of the field to the north of the tower will be three to four times that of the radial distance to the south. For existing plants, the ratio is of the order of 1.5. From an economic point of view, the annual solar energy that can be obtained from the mirror, per unit land area, taking into account PD, is more relevant than solar energy obtained per unit mirror area. These aspects have not been discussed in the available literature. When equal energy contours based on unit land area (taking PD into account) were plotted, the field obtained was similar to that for existing plants. This boundary depends on the PD variation that has been used. Therefore, knowledge of PD variation with r/h is important. These details will be discussed in the next section.

3. Rational Approach to Define the Solar Field Boundary in Non-Dimensional Form

In the case of PT, every trough is equally efficient and therefore the layout of troughs for PT is simple and straightforward. On the other hand, the efficiency of a heliostat depends on the location of individual heliostats relative to the receiver as well as the sun's position. Therefore, the determination of the solar field boundary with respect to the tower is not straightforward in the case of ST. Due to this fact, contours of annual cosine efficiency, annual solar energy per unit mirror area and annual solar energy per unit land area were studied, to see if they can provide any leads.

3.1. Contours of Equal Annual Fractional Cosine Efficiency

Cosine loss arises due to the effective reflection area of the heliostat being reduced by the cosine of the sun's incident angle, θ_i.

Unlike for PT where the cosine effect only depended upon the hour of the day, for ST, it also depends on the location of the heliostat $\left(\frac{x}{h}, \frac{y}{h}\right)$ in the field. Therefore, the cosine effect is different for each heliostat.

In order to calculate the cosine effect, for each hour, the following angles are calculated (all are in degrees):

a) $Declination,\ \delta = 23.45\ \times sin\left\{\left(\frac{360}{365}\right) \times (284 + n)\right\}$ (2)

where n is the day of the year and varies from 1 to 365.

b) $Hour\ Angle,\ \ \omega = 15 \times (t - 12)$ (3)

where t is the hour of the day and varies from 0 to 24

c) $Zenith\ Angle,\ \theta_Z = \cos^{-1}\{(\cos\phi \cos\delta \cos\omega) + (\sin\phi \sin\delta)\}$ (4)

where ∅ is the latitude of the location in degrees.

d) $Altitude\ angle,\ \alpha = 90 - \theta_Z$ (5)

e) $Azimuth\ angle,\ A\text{:}\ \ A^1 = \cos^{-1}\left[\frac{\sin\delta\cos\phi - \cos\delta\sin\phi\cos\omega}{\cos\alpha}\right]$ (6)

$if\ \sin(\omega) > 0,\ A = 360 - A^1,\ else\ A = A^1$

The cosine angle is then calculated as follows:

$$Cosine\ angle,\ \theta_{i,p}\text{:}\ \cos(2\theta_{i,p}) = \frac{\sin\alpha - \frac{x}{h}\cos\alpha\sin A - \frac{y}{h}\cos\alpha\cos A}{\sqrt{1+\left(\frac{x}{h}\right)^2+\left(\frac{y}{h}\right)^2}} \quad (7)$$

$$\cos(\theta_{i,p}) = \sqrt{\frac{1+\cos(2\theta_{i,p})}{2}} \quad (8)$$

The derivation for this can be referred to in (Stine B William, 2001).

To summarise, the $cos\theta$ effect for an ST plant depends on the following:

a) Location of the plant (latitude) which determines the position of the sun at any time of the year
b) The heliostat position $\left(\frac{x}{h}, \frac{y}{h}\right)$ w.r.t the tower
c) The hour of the day

For each point of the field, $\sum_{i=0}^{8760} cos\theta_{i,p}$ is determined. The maximum of this value among all the field points is identified as $\max\{\sum_{i=0}^{8760} cos\theta_{i,p}\}$. Consequently, for each point the fraction $\frac{\sum_{i=0}^{8760} cos\theta_{i,p}}{\max\{\sum_{i=0}^{8760} cos\theta_{i,p}\}}$ is computed and represents the fractional annual cosine efficiency for that point.

Contours of constant fractional annual cosine efficiency are presented in literature (Stine B William, 2001) and can be seen in Figure 4 (Source: http://www.powerfromthesun.net/).

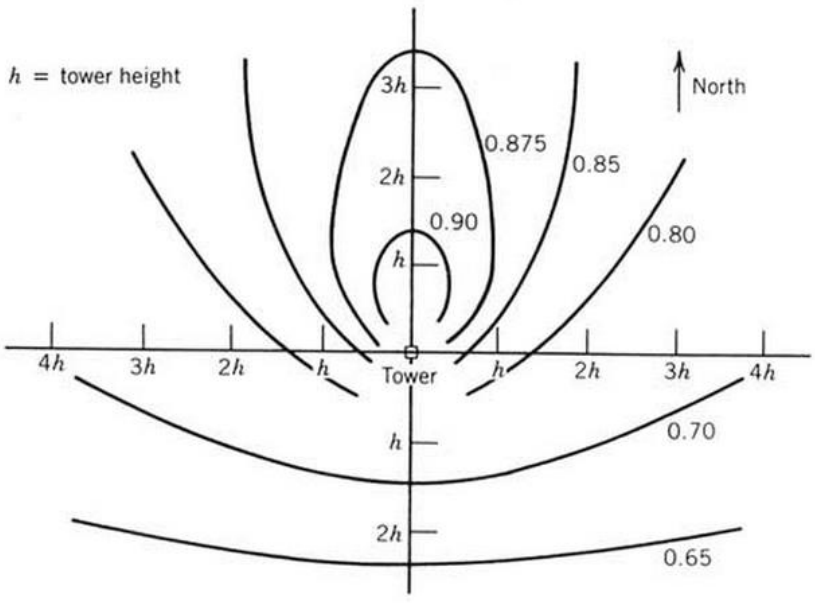

Figure 4: Annual Average Cosine Efficiency at Barstow, California

3.2. Contours of Equal Annual Solar Energy per Unit Mirror Area

It was felt that taking just the annual cosine efficiency was not sufficient, but that this should be coupled with the Direct Normal Irradiation (DNI) data. So the total annual solar energy e_m (Wh/m^2) per mirror area is defined as follows:

$$e_m = \left(\sum_{i=0}^{8760} DNI_i \times cos\theta_{i,p}\right) \quad (9)$$

where subscript i refers to hour and p to the location of the point.

For Seville, Spain, where Gemasolar, PS 10 and PS 20 plants are located, e_m was computed and plotted in the non-dimensionalised base field.

The plot obtained (refer to Figure 5) shows that the contours are oblong. Here the base field was obtained by varying the end limits of x/h and y/h values from -10 to $+10$. The contours are stretched and do not confer with field boundaries (chosen by developers of existing plants) in any way. This shows that this contour, e_m, could not have been used in fixing the maximum field boundary.

Usually, due to slight variations in DNI between morning and afternoon hours, the contours are not exactly symmetrical about the N-S axis. However, the fields are always generally symmetrical. Therefore, while obtaining the contours, the field has been made symmetrical by taking the average value of e_m corresponding to $-x/h$ and x/h for a given y$/h$ point.

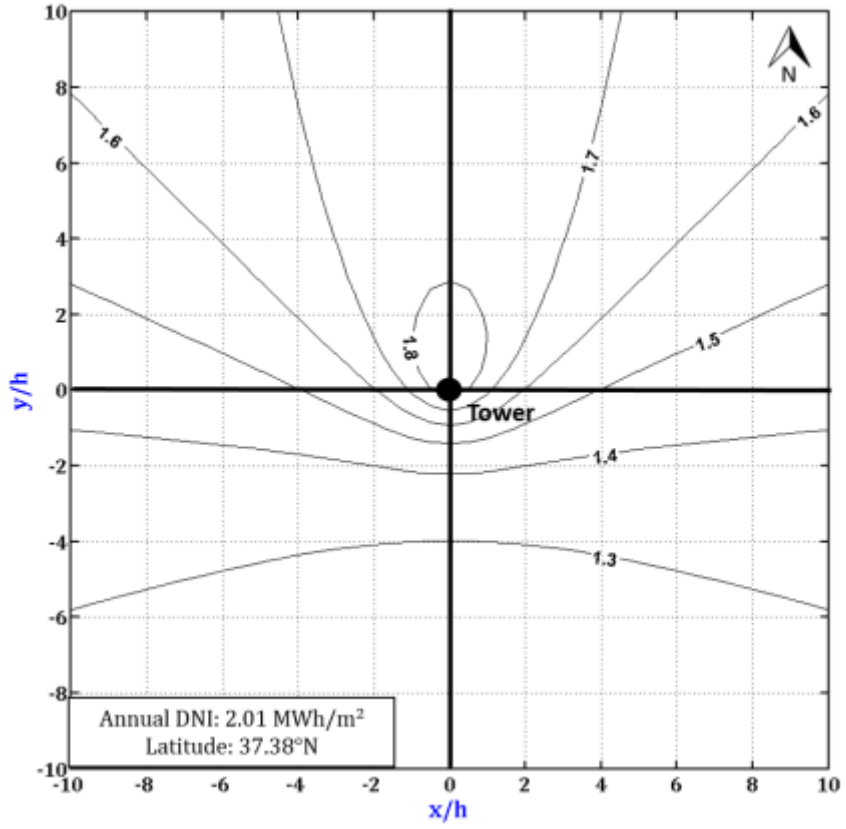

Figure 5: Energy per Unit Mirror Area (e_m) in MWh/m² Contours for Seville

As stated earlier, if PD of the heliostats were same throughout the field, then it would be rational to choose one of these contours as the boundary for the solar field. Since this is not the case, the variation of PD is dealt with in the next section.

3.3. Contours of Equal Annual Solar Energy per Unit Land Area

In reality, heliostats are arranged in a particular layout with gaps between them to allow for shadowing and blocking considerations, maintenance of mirrors etc. Therefore, the assumption that the entire elemental area (covered by the heliostat) reflecting energy, is not valid. The effect of PD will have to be taken into account to see how much elemental area is actually covered with a mirror.

In order to limit the losses due to blockage effects, PD reduces considerably with radial distance from the tower. Figure 6 (Source: http://www.powerfromthesun.net/), shows the variation based on a theoretical layout for solar field. However, the practical significance of this data is unknown. Therefore, the satellite data of the solar fields of available plants were studied to arrive at a nominal variation of PD. The fields of the three ST plants – Gemasolar, PS 10 and PS 20 were studied using Wikimapia, and replicated in excel (See Appendix 1).

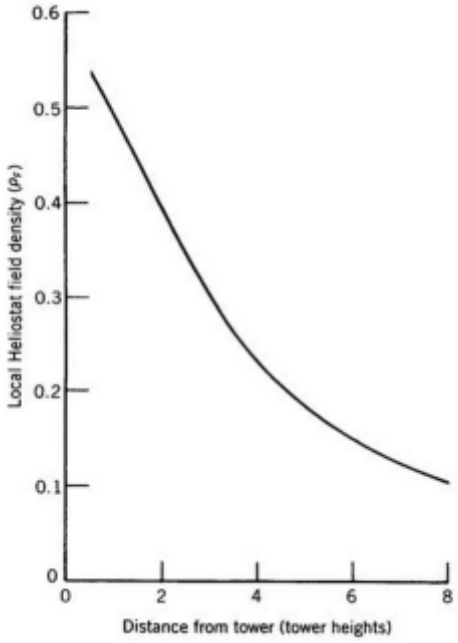

Figure 6: Local Heliostat Density (prediction) for Radial Staggered Field Layouts

From that data a nominal variation of PD vs r/h as given below was determined.

$$PD = 0 \quad \text{for} \quad \frac{r}{h} < \left(\frac{r}{h}\right)_{min}; \tag{10}$$

$$PD = 0.492 - 0.0939\frac{r}{h} \quad \text{for} \quad \left(\frac{r}{h}\right)_{min} \leq \frac{r}{h} \leq 2.8 \tag{11}$$

$$PD = \frac{0.6}{\sqrt{\left(\frac{r}{h}\right)^2 - 1}} \quad \text{for} \quad \frac{r}{h} > 2.8 \tag{12}$$

It was noted that PD was mainly a function of r/h and not dependent on the azimuth angle.

Actual annual reflected energy per unit land area, e_l, at a point p in the base field, taking into account PD is given by:

$$e_l = (PD) \sum_{i=0}^{8760} DNI_i \times cos\theta_{i,p} \quad (13)$$

where PD is the packing density at that point.

A similar exercise, as shown in Section 3.2, was done by plotting contours of e_l. In this case (see Figure 7), the contours are circular.

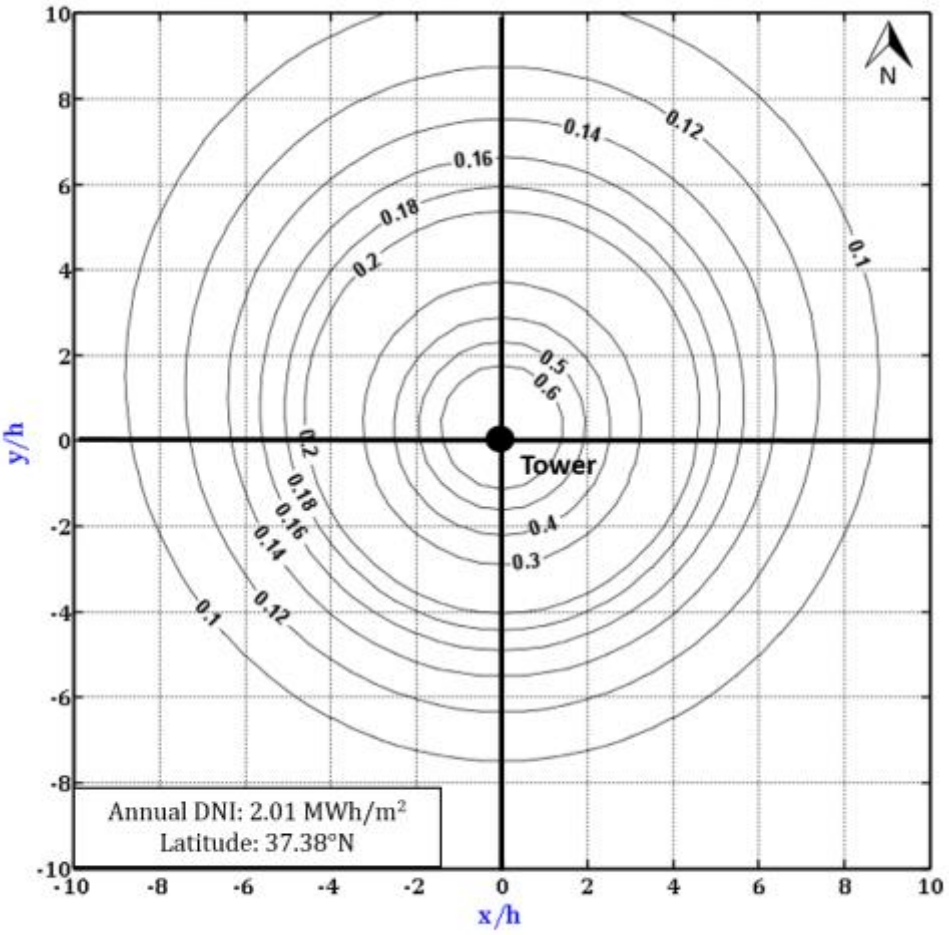

Figure 7: Energy per Unit Land Area (e_l) in MWh/m² Contours for Seville

3.4. Solar Field Boundary in Non-Dimensional Form

By superposing contours of e_l on the actual solar field of these plants, it was inferred that in the general methodology being developed, a contour with a value of $e_l = 0.16$ (MWh/m²) can be used as an initial default value to define the outer solar field boundary. This value can be changed by the user in the programme. For details, see Appendix 2.

Similar to the outer (r/h) boundary (which fixes the maximum limit of the field), there is a limit to the inner r/h value from practical considerations. This can be seen from the images of existing plants as heliostats do not start immediately around the tower. The general trend

observed from existing plants is that $(r/h)_{min}$ varies from 0.5 to 1. The default value chosen for the present programme is 0.5, that is, heliostat rows start at a distance corresponding to half of the height of the tower.

This coupling of the solar field boundary with the height of the tower (taking into account PD of the plant), on a rational basis was a major breakthrough which permits one to design the solar field and corresponding tower height for a CSP plant using ST technology. An overview of the method is presented in the next section.

4. Objective and Overview of the Methodology

Having obtained a rational method of coupling the solar field with the height of the tower, a methodology has been developed for design of the solar field for a CSP plant using ST technology. This methodology is similar to that developed for designing a solar field of PT technology (MA Ramaswamy V. C., 2012).

4.1. Objective

Given, the location of the plant and corresponding DNI data, the capacity of the plant, number of thermal energy storage hours, maximum fraction of hybridisation permitted and efficiencies of various components associated with an ST plant, the objective of the methodology is to arrive at the optimum solar field, which would give the maximum annual solar to electric conversion efficiency. Later on, considering cost and financial aspects, the method would be extended to give the optimum solar field based on LCOE. An overview of the methodology is given as follows.

4.2. Overview

1. Considering the location of plant and DNI data for that location, the solar field boundary in non-dimensional form in terms of $(x/h, y/h)$ or $(r/h,\theta)$, taking default values or user defined values for $\left(\frac{r}{h}\right)_{min}$ and annual solar energy per unit land area, e_l in MWh/m^2, the non-dimensional boundary of the field is determined.
2. For the specified design capacity, the rated power that is required from the solar field, $P_{s,d}$, is calculated taking into account efficiencies of the receiver, heat exchanger and power block.
3. The height of the tower, and corresponding solar field for SM=1 is determined by equating the power generated by the solar field at the best of the 8760 hours in the TMY to the design thermal power from the solar field. In determining e_l, the attenuation effects of the reflected rays due to the environment were neglected. For small capacity plants of the order of 1 MW or less, attenuation effects could be perhaps neglected and the height corresponding to the solar field for SM=1, $h[1]$, can be directly determined. However, in general, $h[1]$ is determined by iteration.
4. The height for a given SM, $h[SM]$, is computed as $h[SM] = h[1] \times \sqrt{SM}$. This is done for SMs ranging from 1 to 4 in suitable steps. For each SM, the solar energy generated by the field and the electrical energy generated by the plant is calculated by taking into consideration the efficiencies of the receiver, heat exchanger and power block and also the energy directed to/taken from the thermal storage block and energy used from hybridisation.
5. The optimum height and solar field for a given storage capacity and hybridisation is determined based on maximum solar to electric conversion efficiency, η_{s-e}, (from a technical point of view). The optimum height and solar field can also be determined by

considering the minimum LCOE condition if the cost and financial parameters are known. In the present study, optimum SM is determined from the consideration of maximum η_{s-e}. It will be extended to consider the LCOE in subsequent studies.

5. Detailed Explanation of Methodology

In this section, the detailed steps of the methodology for conducting a technical analysis are discussed.

5.1. ST Input Data

Input data on the ST plant used in this methodology are listed below.

5.1.1. Plant Data

ST plant data for which the methodology is applied are given below:

a) **Location** – this includes the hourly Direct Normal Irradiance (DNI) data (for 8760 hours) in W/m^2 and the latitude (ϕ) of the plant in degrees.
b) **Plant capacity** ($P_{cap,d}$) in MW – the design/rated capacity of the plant.
c) **Storage hours** (t_s) in hours - this comes into the picture if the plant has a thermal energy storage component.
d) The **fraction of hybridisation** (f_{hb}) - the maximum fraction of design energy which is permitted as the hybridisation component.

5.1.2. Data needed for Determining the Solar Field Boundary

a) **Minimum non-dimensional distance from tower** $\left(\frac{r}{h}\right)_{field\ min}$. This is the non-dimensionalised radial distance at which the first row of heliostats around the tower is located.
b) **Non-dimensional length/width of elemental area** $\left(\frac{d_x}{h}\ or\ \frac{d_y}{h}\right)$ – The non-dimensionalised coordinates are varied in steps of $\frac{d_x}{h}$ or $\frac{d_y}{h}$ across the field in order to determine e_l contours. The choice of e_{lf} determines the non-dimensional solar field outer boundary. In the present model, x/h and y/h values are varied from $(-10,-10)$ to(10,10) in steps of $\frac{d_x}{h}\ or\ \frac{d_y}{h}$ by sweeping y/h for each step of x/h. The default value for $\frac{d_x}{h}\ and\ \frac{d_y}{h}$ is taken as 0.25.

5.1.3. Data on Efficiencies of Various Components of the ST Plant

a) **Reflectivity of heliostats** (ρ) – the fraction of energy incident on the heliostat that is reflected onto the receiver.
b) **Attenuation factor** – Two models have been considered, Clear or Hazy day, depending on the conditions of the atmosphere for the attenuation effect.
c) **Receiver efficiency** ($\eta_{receiver}$) – the ratio of energy gained by the HTF to the energy incident on the receiver surface.
d) **Heat exchanger efficiency** (η_{he}) – the ratio of energy gained by the working fluid to the energy input from the HTF.
e) **Thermal storage efficiency** (η_{st}) – the ratio of the thermal energy stored to the thermal energy input to the storage system.

f) **Power block efficiency** (η_{pb}) – the total efficiency of various components (turbine, condenser, de-aerator, pumps etc.) of the power block.

In the present report, the scope is limited to the use of a steam Rankine cycle to run the power block. The power block efficiency depends on many factors, for example, the inlet pressure and temperature of steam, condenser pressure, capacity of power block and mass flow rate of steam (MA Ramaswamy V. C., 2012). The variation of gross maximum power block efficiency with the turbine inlet temperature for different turbine outlet temperatures, (MA Ramaswamy V. C., 2012), is shown in Figure 8 (Source: Engineering Economic Policy Assessment of Concentrating Solar Thermal Power Technologies for India, 2012).

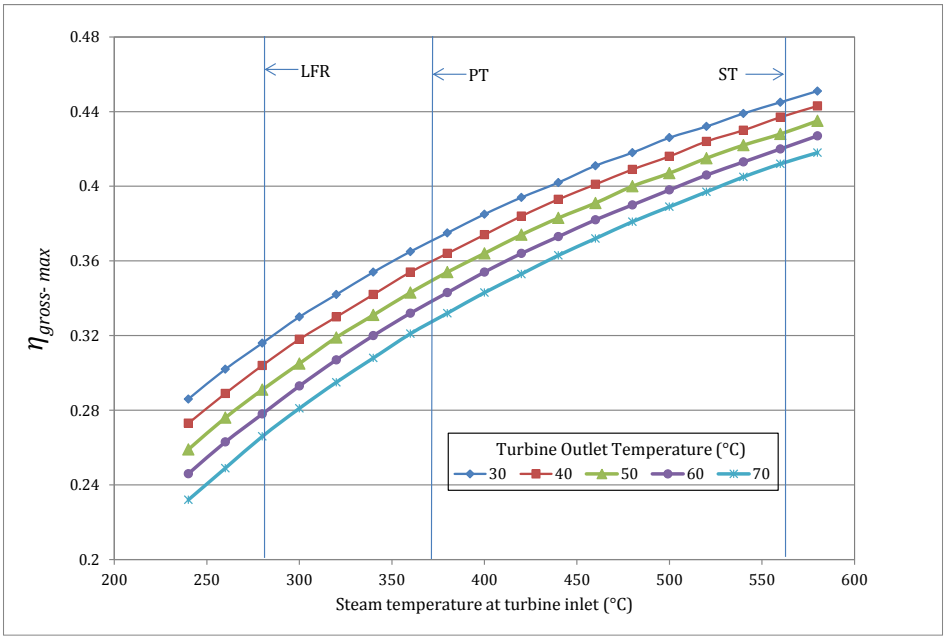

Figure 8: Variation of Gross Maximum Efficiency with Turbine Inlet Temperature

As can be seen from Figure 8 for ST a value of around 44.1% is taken as the maximum possible power block efficiency that can be attained (at utility scale of 50 MW and turbine outlet temperature of 70°C). The actual power block efficiency for capacities lesser than 50 MW plants η_{actual} is computed based on the following relations (ITP, 2012):

$$\eta_{rel} = \left(1 - 0.59 \times e^{(-0.06 \times P_{cap,d})}\right) \text{ and } \eta_{rel} = \frac{\eta_{actual}}{\eta_{gross-max}} \quad (14)$$

where $P_{cap,d}$ is the design plant capacity in MW.

Hence the final power block efficiency conditions (which has been used in this model) are as follows:

$$\eta_{pb} = 0.441 - 0.262 \times e^{-0.06 \times P_{cap,d}} \quad for \;\; 0 \leq P_{cap,d} < 50 \quad (15)$$

$$\eta_{pb} = 0.44 \quad for \;\; P_{cap,d} \geq 50 \quad (16)$$

In the Graphical User Interface (GUI) tool developed for ST, all the inputs mentioned above can be varied by the user depending on the plant configuration and requirement. Default values have been built into the tool based on a global literature review carried out on various existing ST plants worldwide (MA Ramaswamy T. N., 2014).

5.2. Determination of Non-dimensional Solar Field Boundary and Number of Field Points within Boundary

The values of x/h and y/h are varied from $(-10, -10)\ to\ (10,10)$ in steps of non-dimensional interval $\left(\frac{d_x}{h} or\ \frac{d_y}{h}\right)$ by sweeping y/h for each step of x/h. This number (maximum field coordinate) can be increased or decreased in the code by the user if necessary. The number 10 has been chosen as the default value because the highest non-dimensionalised radial distance of heliostats $(r/h)_{max}$ of existing plants generally does not exceed 10. The x/h and y/h values are each incremented in steps of the non-dimensional step parameter, $\frac{d_x}{h} or\ \frac{d_y}{h}$. The default step size for this value has been taken as 0.25 but the user has the freedom to choose it.

As described in Section 3.3, the contours of symmetric equal annual solar energy per unit land area e_l are determined.

As described earlier, e_l values for all points in the base field are determined. Then the user can choose the base value for e_l $(e_{lchosen})$ as preferred in order to determine the outer boundary of the solar field.

The default values for $e_{lchosen}$ is 0.16 and $\left(\frac{r}{h}\right)_{field\ min}$ is 0.5. The user has the freedom to change these values.

All the points which have e_l value greater than or equal to $e_{lchosen}$ and r/h value greater than or equal to $\left(\frac{r}{h}\right)_{field\ min}$ are identified. These constitute the field points (the points within this chosen field boundary). The number of points under the field boundary is denoted by N_f.

This non-dimensional solar field boundary depends only on the location of the plant. The advantage of fixing this boundary in terms of tower height, is that, in determining the actual solar field boundary for given specification of an ST plant, only a rational method to determine the tower height is required.

5.3. Determination of Design Solar Power ($P_{s,d}$)

At design conditions, the thermal energy of the HTF $(P_{htf,d})$ at which the plant generates the design electric power is calculated as follows:

$$P_{htf,d} = \frac{P_{cap,d} \times 10^6}{\eta_{pb} \times \eta_{he}} \qquad (17)$$

where $P_{cap,d}$ is the design electrical capacity of the plant in MW, η_{pb} is the power block efficiency and η_{he} is the heat exchanger efficiency.

The corresponding thermal energy that needs to be collected from the heliostat field ($P_{s,d}$) is calculated as follows:

$$P_{s,d} = \frac{P_{htf,d}}{\eta_{receiver}} = \frac{P_{cap,d} \times 10^6}{\eta_{receiver} \times \eta_{he} \times \eta_{pb}} \quad (18)$$

5.4. Determination of Height of the Tower at SM=1

The steps to determine the height of the tower at SM=1 is given in this section.

Since the non-dimensional solar field boundary has been chosen, and N_f has been determined, the solar power that is impinging on the receiver from the field for any hour (i of the year) is calculated using the following equation.

$$P_i = \left(\left(\frac{d_x}{h} \times \frac{d_y}{h}\right) \times \rho \sum_{j=1}^{N_f} DNI_i \times cos\theta_{i,j} \times PD \times \eta_{att,j}\right) \times (h)^2 \quad (19)$$

where, $\eta_{att,j}$ is the attenuation efficiency at point j. It depends on whether a clear day model (Equation 20) or a hazy day model (Equation 21) is used (Stine B William, 2001).

$$\text{For clear day: } \eta_{att,j} = 0.99326 - 0.1046 S_{n,j} + 0.017 {S_{n,j}}^2 - 0.002845 {S_{n,j}}^3 \quad (20)$$

or

$$\text{For hazy day: } \eta_{att,j} = 0.98707 - 0.2748 S_{n,j} + 0.03394 {S_{n,j}}^2 \quad (21)$$

where $S_{n,j}$ is the slant height of the point, j, from the top of the tower in km and is given by Equation 22.

$$S_{n,j} = \left(\sqrt{(x)^2 + (y)^2 + (h)^2}\right)/1000 \quad (22)$$

As can be seen, $\eta_{att,j}$ is a function of the height of the tower. The task is to find the value of h, such that the maximum of all 8760 P_i values, P_{imax}, is equal to $P_{s,d}$.

Since it is an implicit equation, h has to be determined by iteration.

First the initial value of h at SM=1, $h[1]$, is determined by taking $\eta_{att,j} = 1$ (zero attenuation condition). Then,

$$h[1] = \sqrt{\frac{P_{s,d}}{\left(\frac{d_x}{h} \times \frac{d_y}{h}\right) \times \rho \sum_{j=1}^{N_f} DNI_i \times cos\theta_{i,j} \times PD_j \times 1}} \quad (23)$$

If P_{imax} is calculated with this value of h (considering attenuation), it will naturally be lesser than $P_{s,d}$.

Therefore, a numerical iterative procedure is used for incrementing $h[1]$ in steps of Δh to give $h_{new}[1]$. Δh is initially taken to be 5 m and subsequently reduced to $\Delta h = 0.1\ m$, such that for a particular value of $h_{new}[1]$, $P_{imax} \leq P_{s,d}$ and for $(h_{new}[1] + 0.01)$, $P_{imax} > P_{s,d}$. The lower value,

that is, $h_{new}[1]$ is taken as the height of the tower for SM=1 condition and the corresponding field is determined.

If this tower height and corresponding solar field is used, the design power is generated by the ST plant just for a brief period corresponding to the hour that provides $P_{i,max}$. At all other hours, the power generated will be much less than the rated capacity, such that the overall efficiency of the plant is poor. Therefore, one needs to determine the annual energy generated by the ST plant (considering thermal storage and hybridisation) for different solar field areas, gradually increasing it from that corresponding to SM=1 and determine the optimum value of SM for which the annual solar to electric conversion efficiency is maximum. These details are covered in Section 5.5.

5.5. Determination of Hourly Solar Power from the Field to the Heat Exchanger

The field area is in terms of non-dimensional r/h contours, and PD is also a function of r/h. The mirror area and field area are proportional to h^2. So, the mirror area cannot be increased without increasing the value of h.

Therefore, the height of the tower at any SM, $h[SM]$, is taken to be as follows:

$$h[SM] = h[1] \times \sqrt{SM} \tag{24}$$

Based on the attenuation model chosen, $\eta_{att,j}$ is obtained for each point.

Now the actual power that is input to the heat exchanger is computed for each hour of the year using Equation 25.

$$P_{htf,i} = \left(\left(\frac{d_x}{h} \times \frac{d_y}{h}\right) \rho \times \eta_{receiver} \sum_{j=1}^{N_f} \mathrm{DNI}_i \times \cos\theta_{i,j} \times PD \times \eta_{att,j}\right) \times h[SM]^2 \tag{25}$$

The solar thermal power generated at hour i, $P_{htf,i}$, given by Equation 25, may be lower or higher than $P_{htf,d}$, the design solar thermal power needed to generate the rated electrical power. The power plant is generally permitted to operate at 10% overload. Therefore solar thermal power corresponding to $(1.1 \times P_{htf,d})$ can be utilised to generate the electrical power. If hybridisation is permitted and if $P_{htf,i}$ is less than $(1.1 \times P_{htf,d})$, then hybridisation can be used to augment $P_{htf,i}$ to increase the electrical power output. On the other hand, if $P_{htf,i}$ is greater than $(1.1 \times P_{htf,d})$ (as can happen for higher values of SM) and if thermal storage is utilised, the excess solar power can be directed to the thermal storage block (if it is not full). If thermal storage is full, the heliostats have to be defocussed to limit $P_{htf,i}$ to $(1.1 \times P_{htf,d})$.

Therefore, electrical power generated at any hour has to be computed taking the above factors into consideration. These details are covered in Section 5.6.

5.6. Computation of Electrical Energy generated

The procedure for computing electrical energy is identical to that which was used in the CSTEM tool for PT (MA Ramaswamy V. C., 2012). For the sake of completeness, it is given in this section.

Inputs:

1) $P_{htf,d}$ is calculated
2) Storage hours (t_s)
3) The maximum amount of energy that can be stored is calculated:

$$E_{tes,max} = \frac{P_{htf,d} \times t_s}{\eta_{st}} \quad (26)$$

where $P_{htf,d}$ is the design capacity in MW, t_s is the number of storage hours and η_{st} is the storage heat exchanger efficiency

4) The thermal stored energy available E_{tea} is initialised to zero
5) The fractional thermal power from the solar field is $f_{th} = P_{htf,i}/P_{htf,d}$
6) When $P_{htf,i} = P_{htf,d}$, then f_{th} is denoted by $f_{th,d}$ (the design fraction of thermal energy with the HTF). Its value is 1
7) The plant is assumed to operate at 10% overload condition. So, $f_{th,max}$ is 1.1.
8) $f_{th,min}$, the minimum value of f_{th} below which the plant is shutdown, is taken as 0.25
9) f_{hb}, as already discussed, refers to the maximum fraction of thermal power that can be delivered through hybridisation. This limits the capacity of the natural gas burner. The natural gas burner will be designed such that it delivers $f_{hb} \times P_{htf,d}$ amount of power
10) L_f, Loss Factor, is defined as the fraction of electrical energy lost per hour of shutdown of the plant, to energy that the plant would have generated in 1 hour of operation at design capacity. The energy lost is $L_f \times t_{shutdown} \times P_{cap,d}$ where $t_{shutdown}$ is the hours for which the plant has been shutdown and $P_{cap,d}$ is the design capacity

Procedure:

1) For a chosen SM, the corresponding $P_{htf,i}$ is calculated (as explained in Section 5.5) for each hour of the year.
2) Start from 1st January and for each of the 8760 hours of the year, the electrical energy generated is computed as shown in the following steps.
3) The fractional solar thermal power $f_{th,s}$ is given by $P_{htf,i}/P_{htf,d}$.
4) Initially f_{th} is taken as equal to $f_{th,s}$.
5) Once the available f_{th} from solar field is known, the following steps are applied:

a. Check if $f_{th} \geq f_{th,max}$

If so, stored energy increases

- $E_{tea} = E_{tea} + (f_{th} - f_{th,max})\, P_{htf,d} \times \Delta t \times \eta_{st}$ (Δt *is taken as* 1 *hour*)
- If $E_{tea} \geq E_{tea,max}$, then $E_{tea} = E_{tes,max}$

If $E_{tea} \geq E_{tea,max}$, then some heliostats will have to be defocussed in order to limit $f_{th,s}$ to $f_{th,max}$, since excess solar energy cannot be stored beyond its maximum capacity.

Maximum fractional power available from stored energy, $f_{th,sta} = \frac{E_{tea} \times \eta_{st}}{P_{htf,d} \times \Delta t}$.

The fraction of thermal energy available to power block $f_{th} = f_{th,max}$ and the electrical energy for that hour (e_g) is calculated. In this case, $f_{hb,used}$ is zero.

b. If $f_{th} < f_{th,max}$ then compute $f_{th,m}$, the modified f_{th} ,as follows

- $f_{th,m} = f_{th} + f_{th,sta}$
- Check if $f_{th,m} \geq f_{th,max}$

b1. If $f_{th,m} \geq f_{th,max}$ then

Fraction of thermal power used from storage: $f_{th,st} = f_{th,max} - f_{th}$

Fraction remaining in storage: $f_{th,sta} = f_{th,sta} - f_{th,st}$

Stored energy available is updated: $E_{tea} = \frac{f_{th,sta} \times P_{htf,d} \times \Delta t}{\eta_{st}}$.

Fraction of thermal power available to power block $f_{th} = f_{th,max}$.

Electrical energy output , e_g, for that hour is calculated.

In this case, $f_{hb,used}$ is zero.

b2. If $f_{th,m} < f_{th,max}$, then the fraction of the total thermal power that can be delivered including hybridisation is calculated, $f_{th,T} = f_{th,m} + f_{hb}$.

- Again if $f_{th,T} \geq f_{th,max}$, then $f_{hb,used} = (f_{th,max} - f_{th,m})$ and $f_{th} = f_{th,max}$. Electrical energy e_g for that hour is calculated. Stored energy available is updated: $E_{tea} = \frac{f_{th,sta} \times P_{htf,d} \times \Delta t}{\eta_{st}}$.
- If $f_{th,T} < f_{th,max}$, then $f_{th} = f_{th,T}$ and $f_{hb,used} = f_{hb}$. Stored energy available is updated: $E_{tea} = \frac{f_{th,sta} \times P_{htf,d} \times \Delta t}{\eta_{st}}$. Electrical energy e_g for that hour is calculated.

b3. If $f_{th,T} < f_{th,min}$ then $f_{th} = 0, f_{th,st} = 0$ *and* $f_{hb,used} = 0$ electrical energy generated is taken as 0. The plant is considered to be non-operational for that Δt .

6) The partial load of the power block (MA Ramaswamy V. C., 2012), f_p, is found from the analytical expressions:

- $f_p = 0$ for $f_{th} < f_{th,min}$;
- $f_p = 0.12 + 1.1 \times (f_{th} - 0.2)$ for $f_{th,min} < f_{th} < 1$;
- $f_p = f_{th}$ for $f_{th} > 1$;

7) The maximum gross electrical energy that is generated during Δt is given by $e_g = f_p \times P_{g,d} \times \Delta t$,

where Δt is 1 hour, $P_{g,d}$ is the design capacity in W $(= P_{cap,d} \times 10^6)$.

8) When the plant is not operating, the equivalent accumulated electrical energy lost due to thermal losses for that Δt is given by $e_{start} = e_{start} + L_f \times P_{g,d} \times \Delta t$.

9) Therefore, the actual electrical energy generated (e_{ga}) is given by the following condition:

- If $e_g = 0$, then, $e_{ga} = 0$, and $e_{start} = e_{start} + L_f \times P_{g,d} \times \Delta t$
- If $0 < e_g < e_{start}$, then $e_{ga} = 0$ and $e_{start} = (e_{start} - e_g)$
- If $e_g \geq e_{start}$, , then $e_{ga} = (e_g - e_{start})$ and $e_{start} = 0$

10) The net electrical energy supplied to grid, e_{grid}, during that interval is equal to $e_{ga} \times (1 - \ Auxiliary\ Power\ Fraction)$. $Auxiliary\ power\ fraction$ is the ratio of power consumed by the auxiliary units to the gross power generated. The default value is taken as 0.1.

11) The electrical energy apportioned to hybridisation (e_{hb}) is $\left(\frac{f_{hb,used}}{f_{th}} \times e_{grid}\right)$ and that apportioned to solar (e_s) is $(e_{grid} - e_{hb})$.

12) On the above basis, the total net electrical energy generated over the whole year can be calculated and also the contributions from solar and hybridisation are separately accounted for.

13) The total annual electrical energy generated $e_{ga,t}$ and annual electricity to the grid $e_{grid,t}$ is computed.

5.7. Computation of Mirror Area, Land Area, *CUF* and $\eta_{s\text{-}e}$

The total Mirror Area (MA) is computed as follows:

$$MA = \left(\sum_{j=1}^{N_f} PD\right) \times \left(\frac{d_x}{h} \times \frac{d_y}{h}\right) \times (h[SM])^2 \quad (27)$$

The total Land Area (LA) is computed as follows:

$$LA = \left\{\left(N_f \times \left[\frac{d_x}{h} \times \frac{d_y}{h}\right]\right) + \left(\pi \times \left(\left(\frac{r}{h}\right)_{field\ min}\right)^2\right)\right\} \times (h[SM])^2 \quad (28)$$

The Capacity Utilisation Factor (CUF) is calculated as follows:

$$CUF = \frac{e_{ga,t}}{P_{g,d} \times 8760} \quad (29)$$

The annual DNI, (DNI_{annual}) in Wh is calculated depending on the location chosen by the user as follows:

$$DNI_{annual} = \sum_{i=1}^{8760} DNI_i \ \times \ \Delta t \quad (30)$$

whereDNI_i is the hourly DNI in W/m^2 and Δt is the time interval depending on the resolution of the data (here taken as 1 hour).

The annual efficiency of conversion from solar to electric energy is computed as follows:

$$\eta_{s-e} = \frac{e_{s,t}}{MA \times (Annual\ DNI)} \quad (31)$$

6. Technical Assessment - Case Study in Jodhpur

In this section, the results of applying the engineering model developed for hypothetical ST plants (located in Jodhpur) are discussed. Jodhpur was chosen because it is one of the locations in India which receives high annual DNI. The parameters chosen for the study are shown in

Table 1.

Table 1: Parameters Considered for Analysis

Parameter	Value Range
Design Capacity (MW)	1,5,10,20,35,50
Hours of thermal storage (t_s)	0,6,15
Fraction of hybridisation (f_{hb})	0,0.1,0.2

For various combinations of these parameters, the CUF, annual solar to electric conversion efficiency and annual electricity generated have been computed for various SM values between one and four in suitable steps.

The results are presented and discussed below.

6.1. No Thermal Storage and no Hybridisation

This section analyses the effect of various plant parameters when no thermal storage or hybridisation is used.

6.1.1. Effect of Capacity of Plant

Table 2 shows the variation of power block efficiency (η_{pb}), mirror area and mirror area per MW corresponding to SM=1 (with no thermal storage and hybridisation).

Table 2: Variation in Power Block Efficiency and Mirror Area for SM=1 with Capacity (t_s=0 and f_{hb} =0)

Capacity (MW)	η_{pb}	Mirror Area at SM = 1 (m^2)	Mirror Area (SM=1) per MW (m^2/MW)
1	0.19	9240	9240
5	0.25	36622	7324
10	0.30	61133	6113
20	0.36	100918	5046
35	0.41	157382	4497
50	0.44	209441	4189

The design efficiency of the power block increases with capacity. Due to this, the mirror area per MW decreases with an increase in capacity. The trend can be observed in Figure 9. It can be noticed that plants with lower capacities will thus have lower overall efficiencies while simultaneously being more expensive.

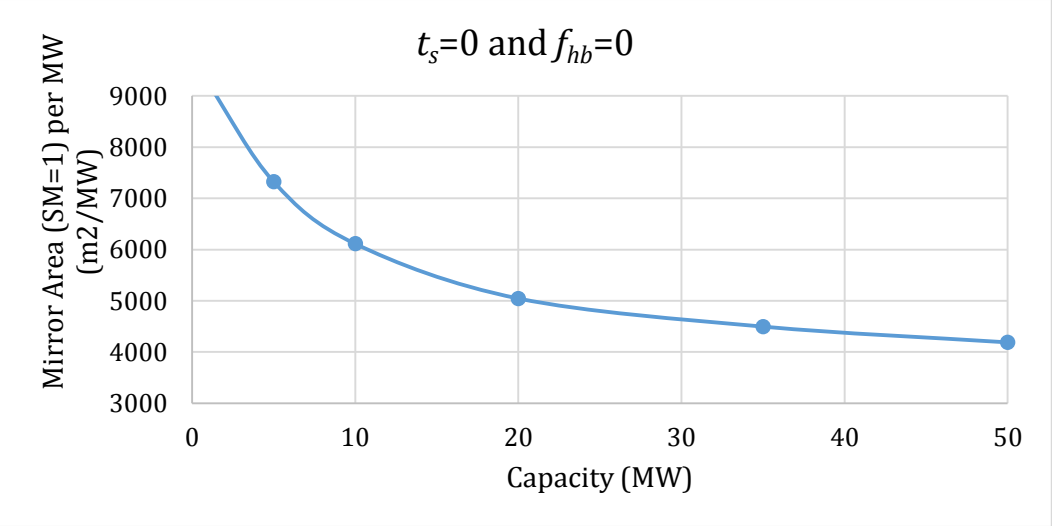

Figure 9: Variation of Mirror Area per MW with Capacity (t_s =0 and f_{hb} =0)

6.1.2. Effect of Solar Multiple

The effect of Solar Multiple on the annual electrical energy generated (for a plant with no thermal storage and hybridisation) is presented in Table 3. At SM=1, the power plant is able to generate power at the design DNI conditions only. However, with increase in SM, the solar field increases and is typically optimised for lowest cost of generation.

Table 3: Annual Electrical Energy Generation with SM for Various Capacities (t_s=0 and f_{hb}=0)

Annual Electrical Energy Generated - MWh (t_s=0, f_{hb}=0)						
SM	**1 MW**	**5 MW**	**10 MW**	**20 MW**	**35 MW**	**50 MW**
1	1617	8082	16169	32335	56600	80847
1.25	2186	10916	21824	43614	76282	108888
1.5	2621	13087	26160	52263	91385	130435
1.75	2907	14513	29008	57964	101335	144654
2	3099	15472	30925	61796	108050	154243
2.5	3342	16687	33355	66659	116562	166398
3	3493	17448	34875	69698	121863	173983
3.5	3597	17961	35903	71746	125465	179131
4	3671	18332	36644	73235	128067	182842

From Table 3, it is seen that for a given SM, the annual electricity generated is proportional to the rated design capacity of the plant.

Therefore, data given in the first column of Table 3 for 1 MW, can be considered as the annual electrical energy generated per MW for all capacities.

To understand the dependency on SM, the variation of annual electrical energy generated per MW of capacity as a function of SM is shown in Figure 10. From this it is clear that the benefits of increasing SM get saturated beyond SM=4.

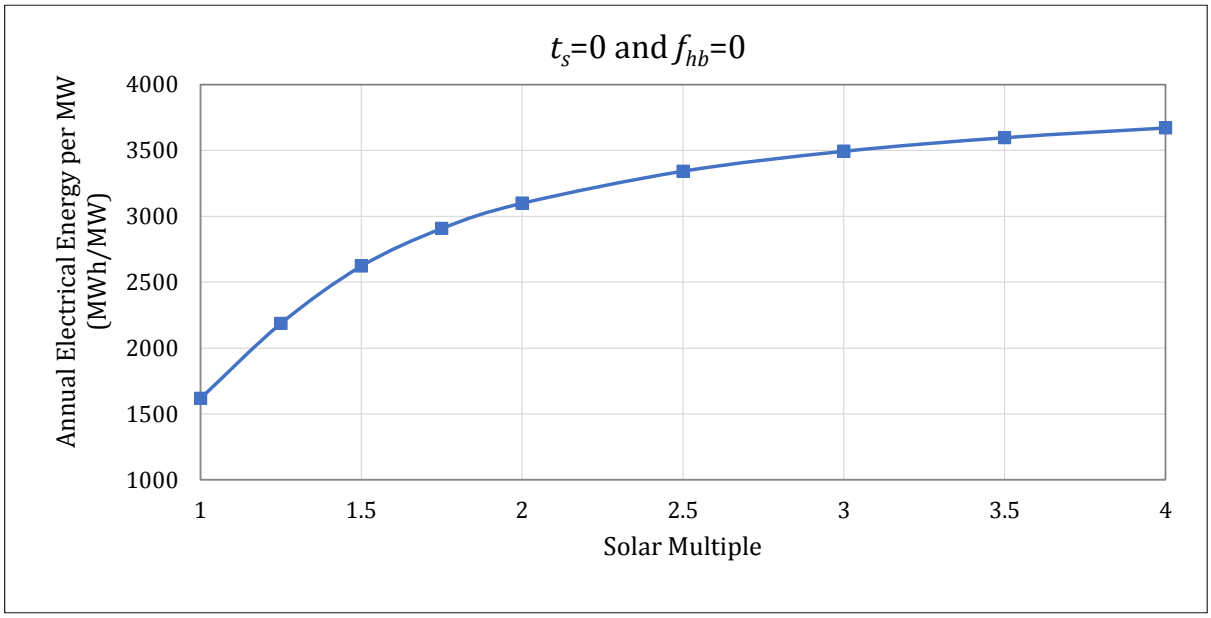

Figure 10: Variation of Annual Electrical Energy per MW with SM (t_s =0 and f_{hb} =0)

Capacity Utilisation Factor (CUF) is the ratio of the actual output from the plant over the year to the maximum possible output from it for that year under ideal conditions. It is given by Equation 29 (given below for reference).

$$CUF = \frac{e_{ga,t}}{P_{g,d} \times 8760}$$

where $e_{ga,t}$ is the total annual gross electricity generated in W and $P_{g,d}$ is the rated gross power in W.

The variation of CUF for all capacities (for no thermal storage and hybridisation) is shown in Figure 11. Here also it is seen that the CUF tends to saturate beyond SM=4.

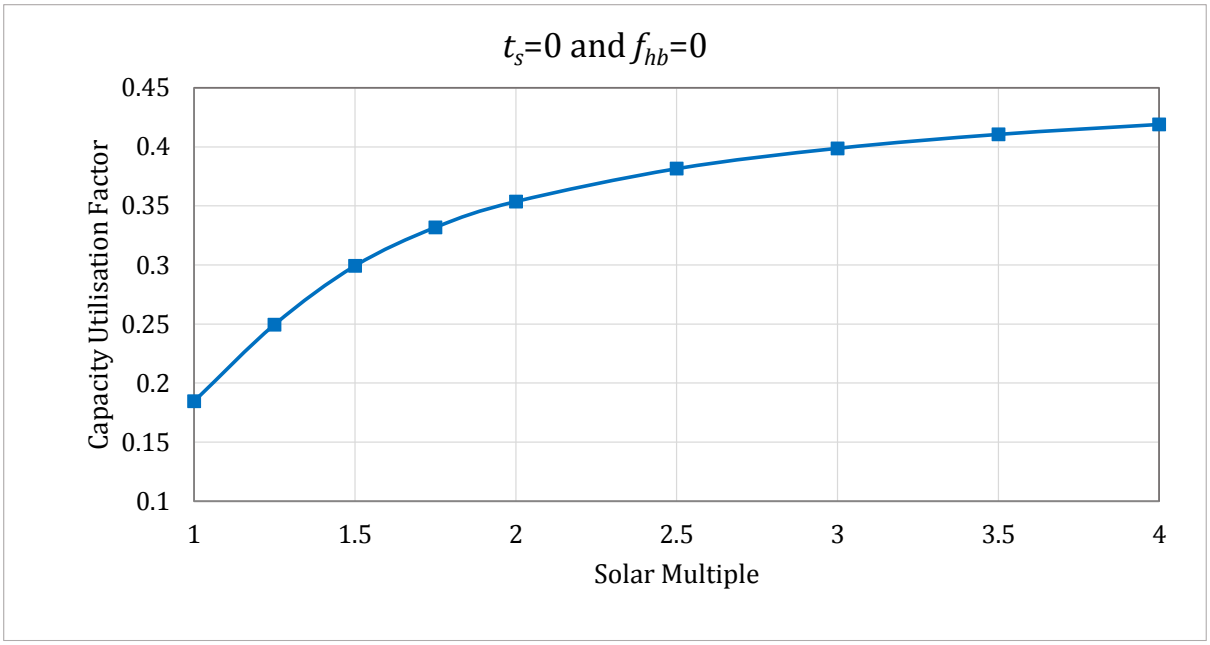

Figure 11: Variation of CUF with SM for all Capacities (t_s =0 and f_{hb} =0)

6.1.3. Annual Solar to Electric Conversion Efficiency

The annual solar to electric conversion efficiency (η_{s-e}) is the ratio of the total annual electricity generated attributed to solar energy to the annual solar energy impinging on the mirrors. It is calculated using Equation 31 (given below for reference).

$$\eta_{s-e} = \frac{e_{s,t}}{MA \times (Annual\ DNI)}$$

where $e_{s,t}$ is the total annual electricity generated that is attributed to solar energy in Wh, MA is the total mirror area of the field in m² and $Annual\ DNI$ is in W/m².

The variation of this quantity with SM (for plants with no storage or hybridisation) has been plotted for various capacities in Figure 12. From this Figure, it can be seen that the maximum efficiency occurs at an SM value of around 1.4 for all capacities and the efficiency increases with capacity reaching a value of about 18% for a 50 MW plant.

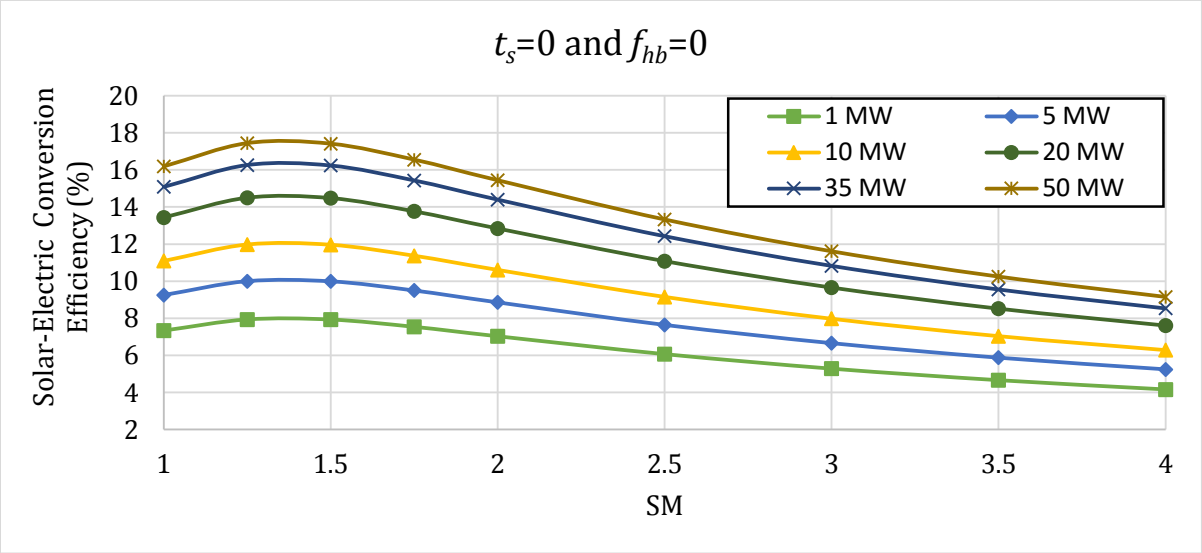

Figure 12: Variation of Annual Efficiency with SM for Various Capacities (t_s =0 and f_{hb} =0)

6.1.4. Electrical Power Generation on a Typical Day

Figure 13 shows the hourly variation of fractional solar power, $f_{th,s}(P_{htf}/P_{htf,d})$, and fractional electrical power f_{pa} (electrical power generated/rated capacity) for January 21st for SM=1 and SM=2 (for a plant without thermal storage and hybridisation).

Note that, $f_{pa} = e_{ga}/P_{g,d}$ and, $f_p = e_g/P_{g,d}$.

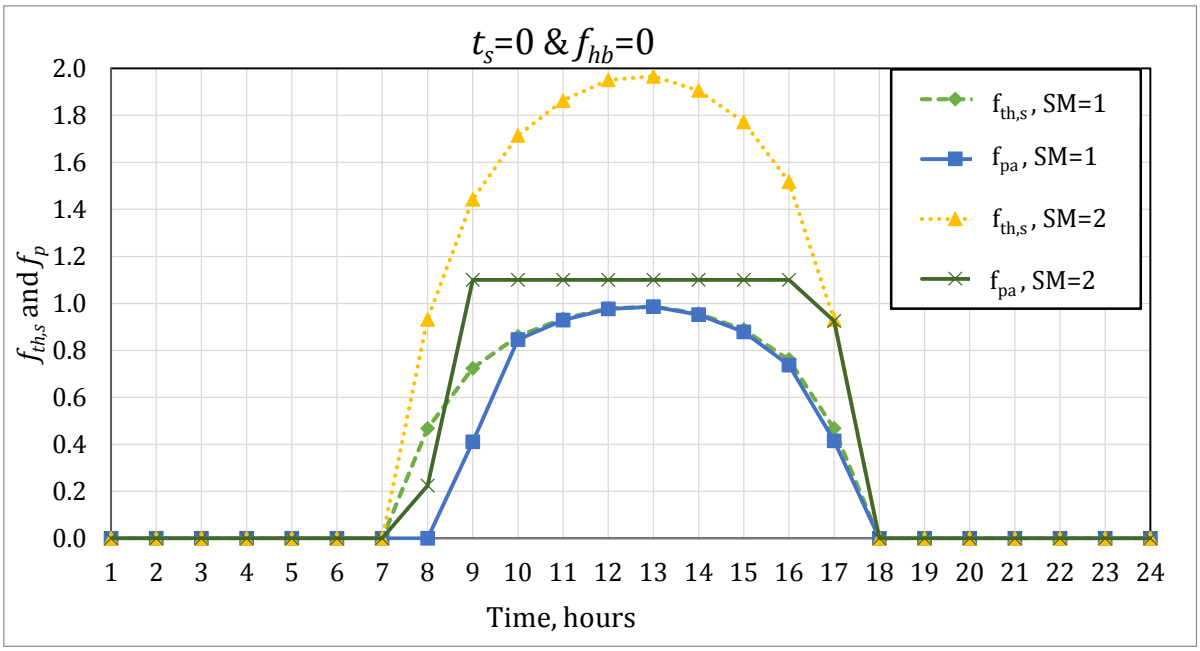

Figure 13: Variation of the Fractional Solar Power and Fractional Electrical Power Generated during a Typical Day (t_s =0 and f_{hb}=0)

The advantage of representing $f_{th,s}$ and f_{pa} is that they are independent of the capacity of the plant.

It can be seen that the lag in electrical power generation as compared to the solar power generation occurs to account for the losses that would have occurred overnight. The solar power generated over the first few hours goes into making up for this lost energy and to make sure the HTF has attained the operating temperature for power generation.

It can be observed that for SM=1, f_{pa} is slightly less than or equal to $f_{th,s}$.

For SM=2, $f_{th,s}$ is almost twice the value corresponding to SM=1. However, f_{pa} does not exceed 1.1 as this is the maximum load condition under which the plant works (10% overload). Therefore, the excess power is not utilised by the power block and some mirrors will have to be defocussed. Essentially, this means that it is not an efficient system.

In these cases, if storage is incorporated, the remaining power generated from the field (after limiting f_p to 1.1), can go into the storage block to be used at times when the power goes below the lowest operating condition.

6.2. Thermal Storage without Hybridisation

In this section thermal storage for three, six and fifteen hours of storage have been considered for plants of capacities 1, 5, 10, 20, 35 and 50 MW. The effect of SM and storage hours on the solar to electric conversion efficiency has been discussed.

6.2.1. Effect of Solar Multiple

The variation in annual energy generated per MW with SM, for thermal storage of zero, six and fifteen hours (for various capacities) and no hybridisation is given in Table 4 and shown in Figure 14.

The variation of CUF with storage (and no hybridisation) is given in Table 5 and Figure 15. The variation of CUF with storage hours for various SMs is also plotted and shown in Figure 16. From these figures one can see that as the number of hours of thermal storage increases, the SM should also be higher (otherwise the system is not efficient). Higher thermal storage hours required, implies that a higher SM needs to be chosen.

Table 4: Variation of Annual Electrical Energy per MW with SM for t_s=0, 6 and 15 hours (f_{hb}=0)

Annual electrical energy in MWh per MW			
SM	**t_s=0**	**t_s=6**	**t_s=15**
1	1617	1617	1617
1.25	2186	2197	2197
1.5	2621	2762	2762
1.75	2907	3314	3314
2	3099	3851	3851
2.5	3342	4745	4905
3	3493	5246	5947
3.5	3597	5519	6928
4	3671	5690	7629

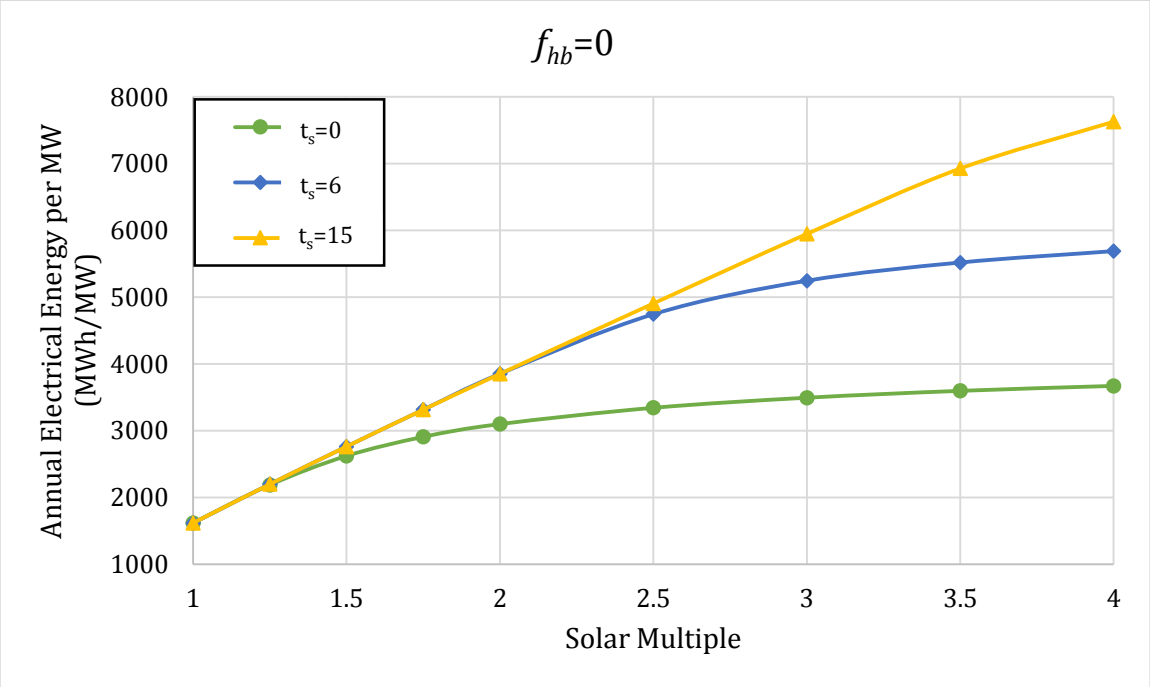

Figure 14: Variation of Annual Electrical Energy/MW with SM for t_s=0, 6 and 15 hours (f_{hb}=0)

Table 5: Variation of Capacity Utilisation Factor with SM for t_s =0, 6 and 15 hours (f_{hb} =0)

Capacity Utilisation Factor (f_{hb}=0)			
SM	**t_s=0**	**t_s=6**	**t_s=15**
1	0.18	0.18	0.18
1.25	0.25	0.25	0.25
1.5	0.30	0.32	0.32
1.75	0.33	0.38	0.38
2	0.35	0.44	0.44
2.5	0.38	0.54	0.56
3	0.40	0.60	0.68
3.5	0.41	0.63	0.79
4	0.42	0.65	0.87

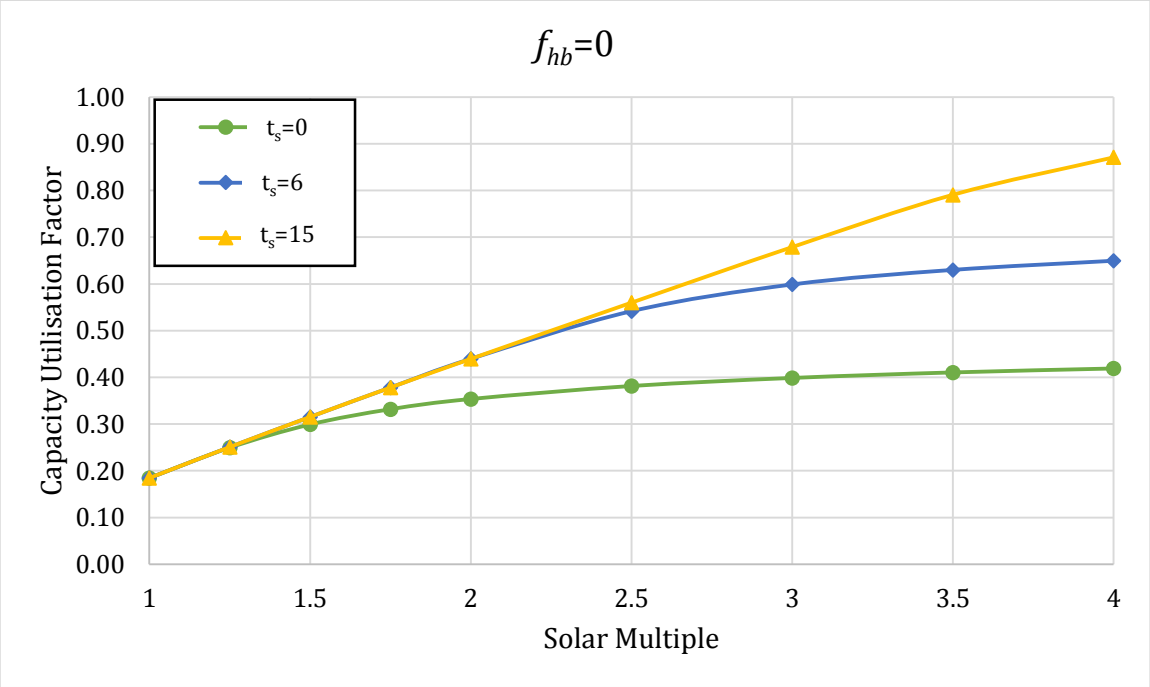

Figure 15: Variation of CUF with SM for t_s=0, 6 and 15 hours (f_{hb} =0)

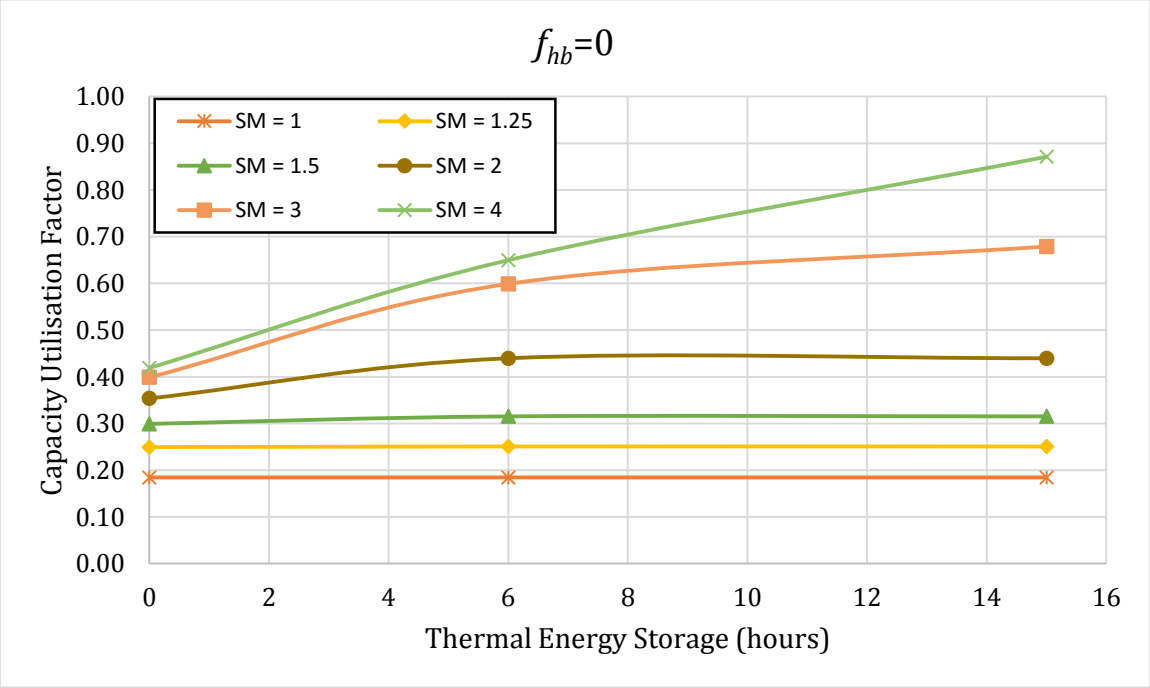

Figure 16: Variation of CUF with Thermal Energy Storage for various SMs (f_{hb} =0)

6.2.2. Annual Solar to Electric Conversion Efficiency

The variation of annual solar to electric conversion efficiency with SM for various capacities (and no hybridisation) is shown in Figure 17and Figure 18 for thermal storage of six and fifteen hours respectively. It is observed that for six hours of storage, the highest efficiency occurs at

SM=2.1 and for fifteen hours of storage it occurs at about SM= 3.2. These are called the optimum efficiency values taking into account the maximum solar to electric conversion efficiency condition. It can also be seen that the overall efficiency increases as the capacity of the plant increases.

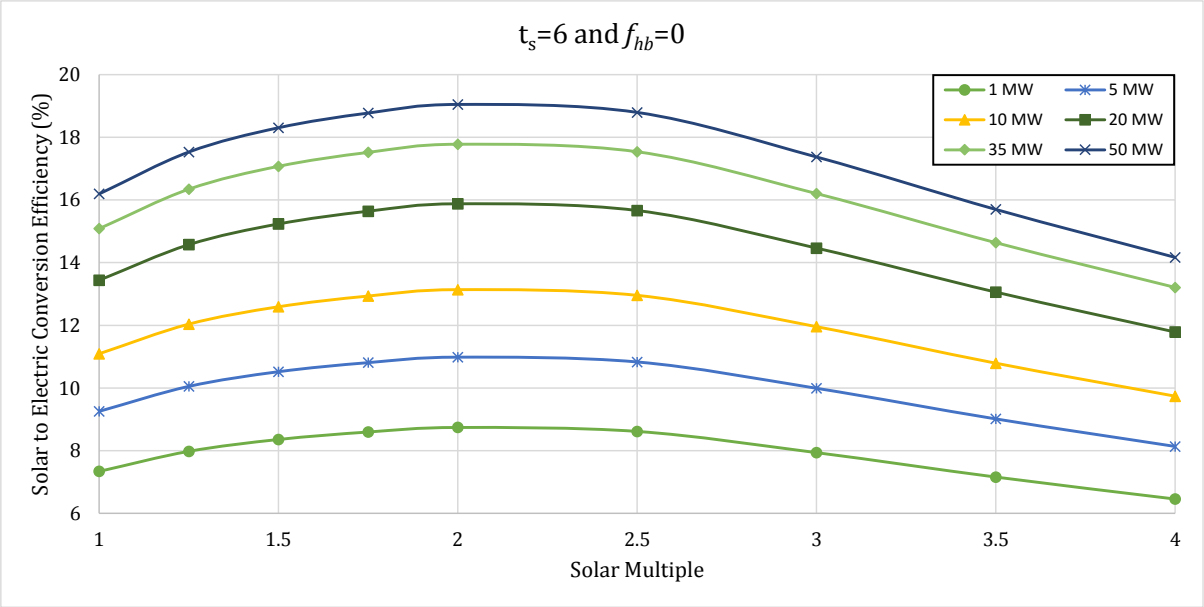

Figure 17: Variation of Solar to Electric Conversion Efficiency with SM for Various Capacities and t_s=6 hours (f_{hb} =0)

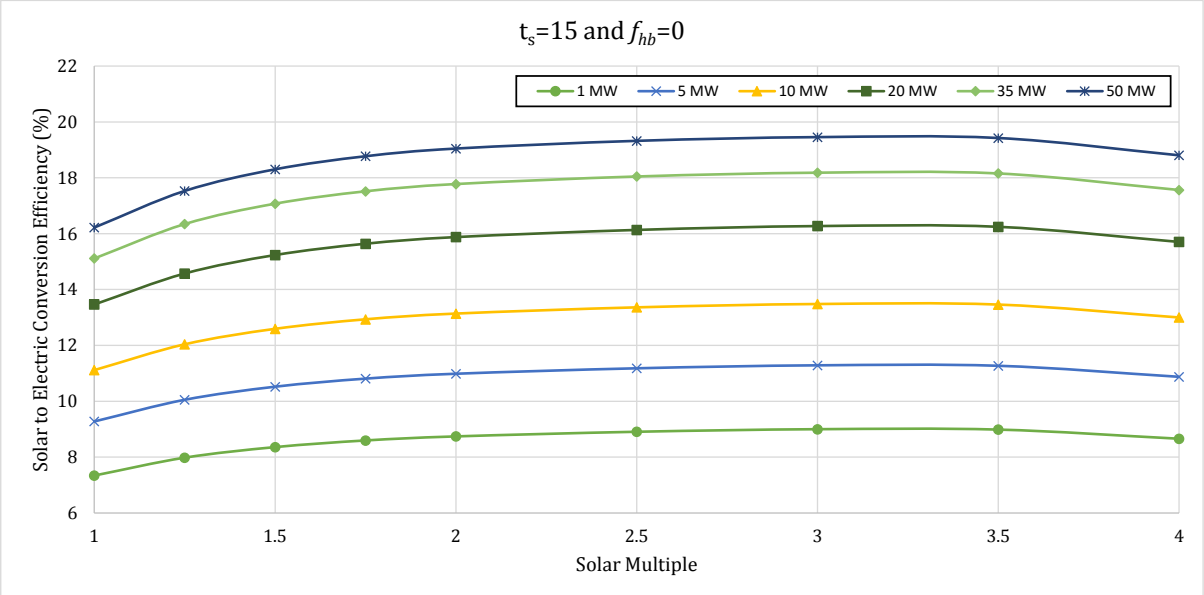

Figure 18: Variation of Solar to Electric Conversion Efficiency with SM for Various Capacities and t_s=15 hours (f_{hb} =0)

6.2.3. Analysis of Performance Parameters at Optimum SM (f_{hb}=0)

Variation of Optimum SM with Storage Hours

Figure 19 shows the variation of the optimum SM as the number of storage hours is increased (with no hybridisation). A linear trend is observed. Optimum SM corresponding to highest η_{s-e} depends only on t_s and not on capacity of the plant.

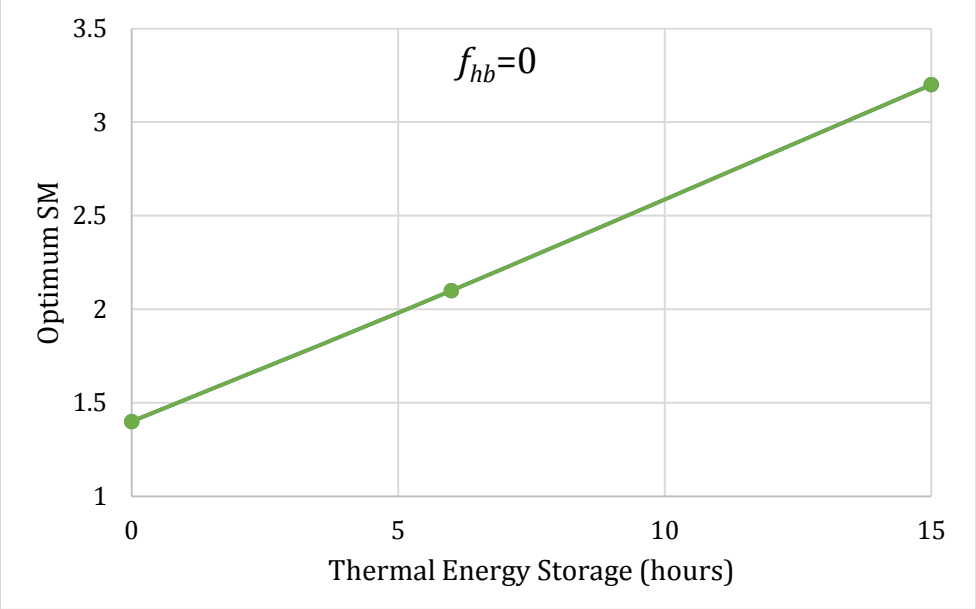

Figure 19: Variation of Optimum SM with Thermal Storage Hours (f_{hb}=0)

Variation of Maximum Annual Efficiency with Plant Capacity

Table 6 shows the variation of maximum annual efficiency of solar to electric energy with capacity for zero, six and fifteen hours of storage (with no hybridisation). The optimum SM values are also indicated next to the t_s values. This information is also shown in Figure 20. It can be seen that the maximum annual efficiency increases with plant capacity as well as storage hours.

Table 6: Variation of Maximum Annual Efficiency with Capacity for t_s=0, 6 and 15 at Optimum SM (f_{hb} =0)

Capacity (MW)	η_{s-e} (%)		
	t_s=0 (SM=1.4)	t_s=6 (SM=2.1)	t_s=15 (SM=3.2)
1	8.01	8.77	9.02
5	10.09	11.03	11.31
10	12.08	13.19	13.51
20	14.62	15.94	16.30
35	16.39	17.84	18.21
50	17.58	19.11	19.48

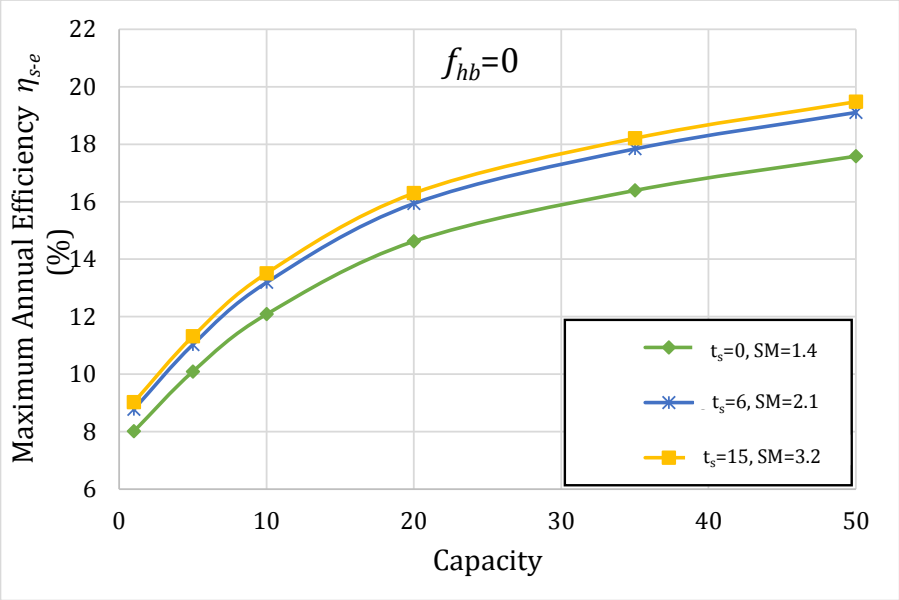

Figure 20: Variation of Maximum Annual Solar to Electric Conversion Efficiency with Plant Capacity for t_s=0, 6 and 15 at Optimum SM (f_{hb} =0)

Variation of Capacity Utilisation Factor with Number of Storage Hours

Table 7 shows the variation of CUF with capacity for zero, six and fifteen hours of storage (with no hybridisation). It can be seen that CUF does not change with capacity for a given number of storage hours but it does change considerably as the number of storage hours are increased. This is also seen in Figure 21 shows the variation of CUF with number of storage hours for 1 MW and 50 MW for $f_{hb} = 0$.

Table 7: Variation of CUF with Plant Capacity for t_s=0, 6 and 15 at Optimum SM (f_{hb} =0)

Capacity (MW)	Capacity Utilisation Factor		
	t_s=0 (SM=1.4)	t_s=6 (SM=2.1)	t_s=15 (SM=3.2)
1	0.282	0.463	0.726
5	0.282	0.462	0.722
10	0.281	0.461	0.719
20	0.281	0.460	0.716
35	0.281	0.458	0.713
50	0.281	0.457	0.711

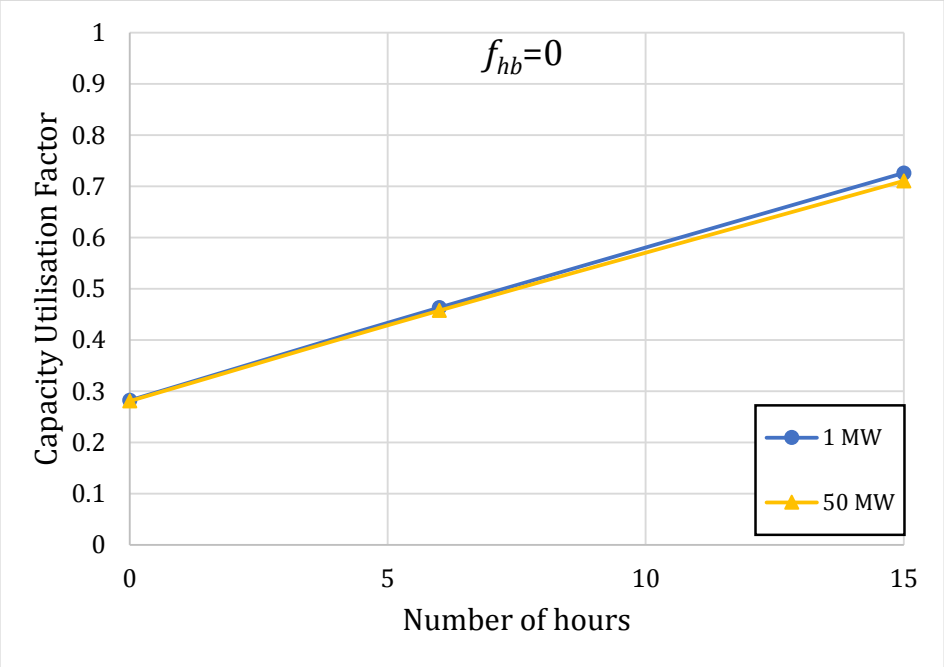

Figure 21: Variation of CUF with Thermal Storage Hours for 1 MW and 50 MW (f_{hb} =0)

6.2.4. Solar Power Input and Electrical Power Generation on a Typical Day

Figure 22 shows the variation of $f_{th,s}$ and f_{pa} over a typical day for SM=2 and 2.5 for six hours of storage (and no hybridisation). From this Figure it can be seen that electrical power is generated for about five hours after sunset for SM=2 and about six hours after sunset for SM=2.5. It can be inferred that as one reaches the optimum SM, it goes to show that the plant can operate for higher number of hours (even after sunset) just from the energy stored. It is to be noted that these inferences should be based on the annual overall efficiency rather than the performance of a single day. This plot has been shown to give a physical idea of how thermal storage works over a typical day of the year and that with a suitable SM, plant operation is feasible even after sunset.

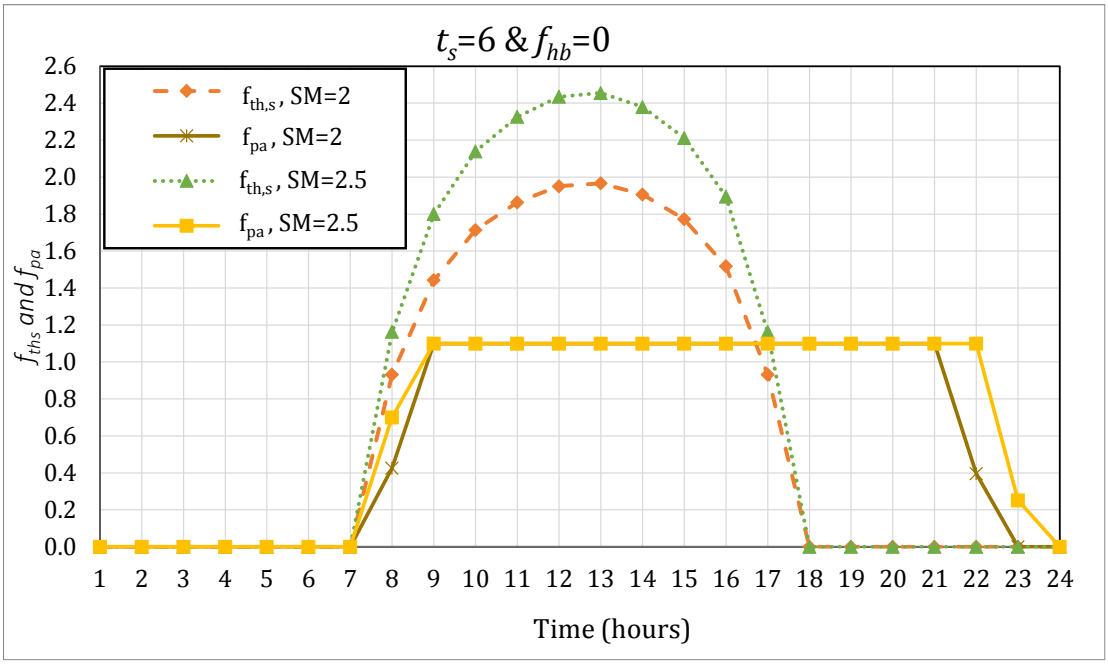

Figure 22: Variation of $f_{th,s}$ and f_{pa} during a Typical Day for t_s =6 hours (f_{hb} =0)

6.3. Hybridisation without Thermal Storage

In this section, the effect of augmenting thermal power to the plant using hybridisation to the extent of 0.1 to 0.2 times the design power required (and zero thermal storage) is discussed.

6.3.1. Effect of Solar Multiple

SM=1

Figure 23 shows the variation of f_{pa} over a typical day for f_{hb}=0, 0.1 and 0.2 along with $f_{th,s}$ for SM=1. Figure 24 gives the value of $f_{hb,used}$ during the day. In all these cases thermal storage is not employed. It can be seen that f_{pa} increases with f_{hb}. For $f_{hb} = 0.1$, $f_{hb,used}$ is the same as f_{hb} throughout the day.

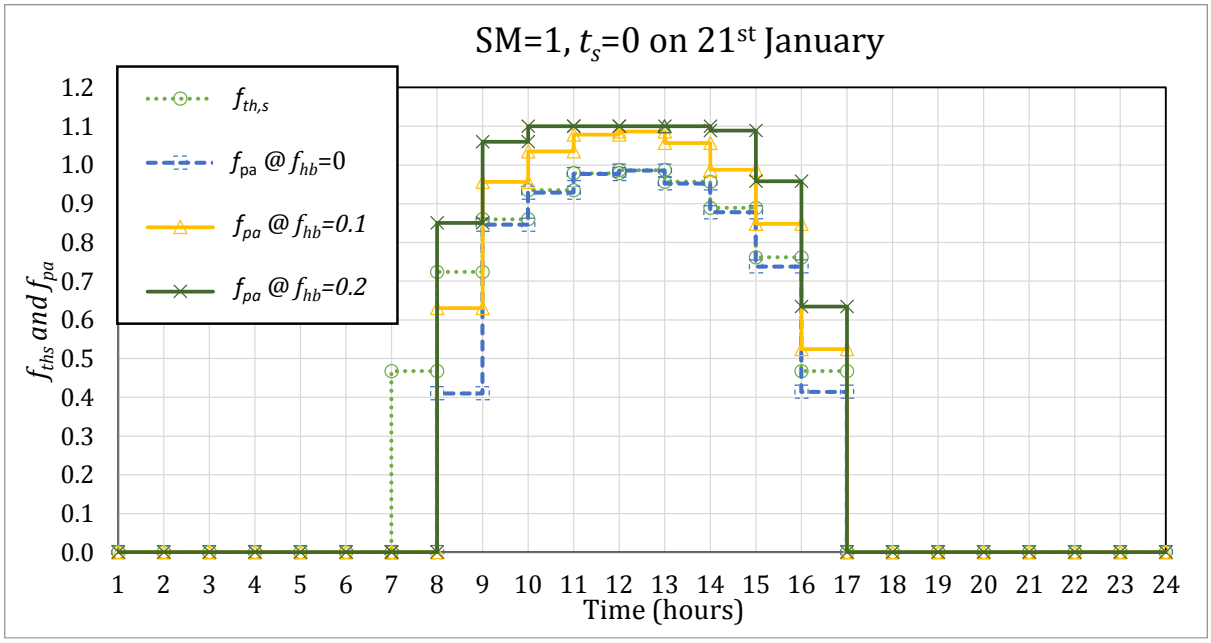

Figure 23: Effect of Hybridisation (f_{hb} =0.1 and 0.2) on the Electrical Power Generated during a Typical Day for SM=1 (t_s =0)

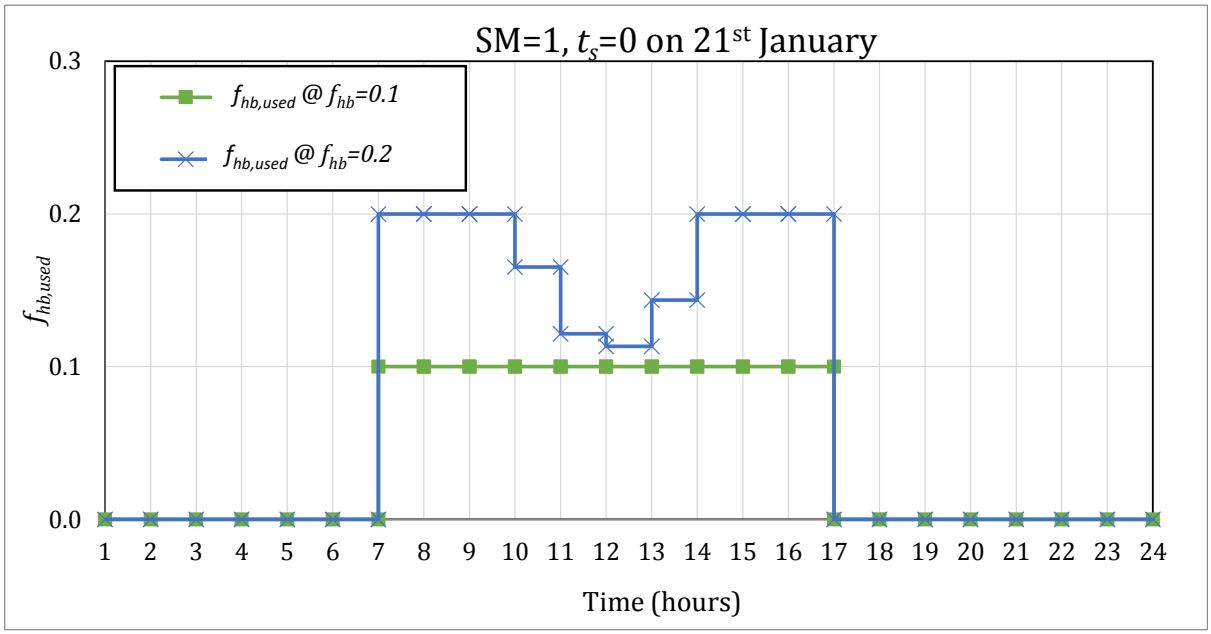

Figure 24: Fraction of Hybridisation Used during a Typical Day for SM=1 (t_s =0)

SM=1.5

Figure 25 shows the variation of f_{pa} over a typical day for f_{hb}=0, 0.1 and 0.2 (with no thermal storage) along with $f_{th,s}$ for SM=1.5. Figure 26 gives the value of $f_{hb,used}$ during the day. It can be seen that, the amount of energy from the field ($f_{th,s}$) is sufficient to run the plant at 1.1 times full capacity for most of the day and hence there is no necessity of hybridisation for most of this period. It is observed that for the first hour $f_{th,s}$ and hybridisation contribute towards making

up of the thermal losses that have occurred overnight. So the amount of energy generated for this hour, f_{pa}, is small. This can be contrasted with the last hour where f_{pa} is not as less as it is for the first hour.

Since hybridisation does not contribute much for SM value of 1.5, higher SMs have not been taken up for analysis.

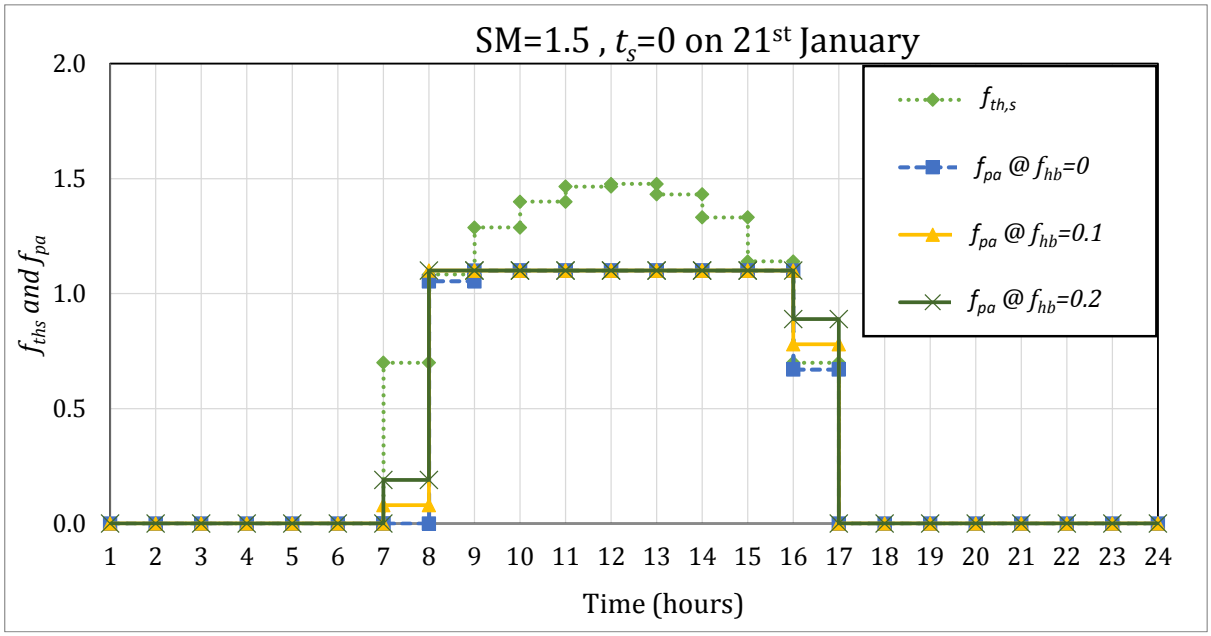

Figure 25: Effect of Hybridisation (f_{hb} =0.1 and 0.2) on the Electrical Power Generated during a Typical Day for SM=1.5 (t_s =0)

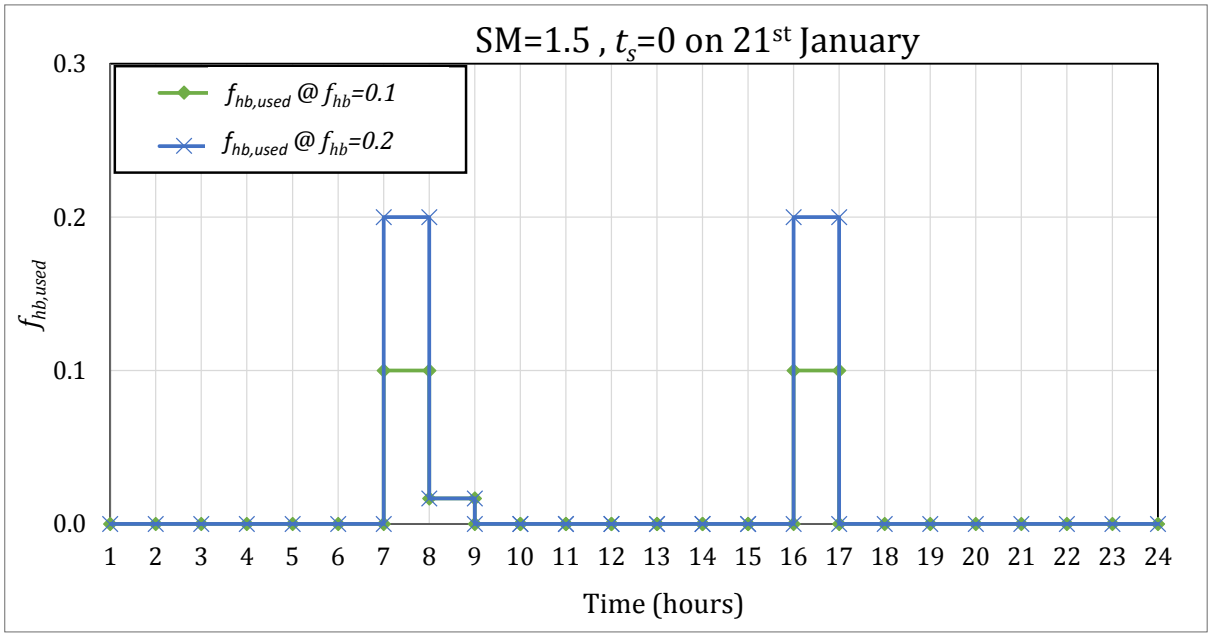

Figure 26: Fraction of Hybridisation Used during a Typical Day for SM=1.5 (t_s =0)

6.3.2. Effect of Hybridisation Factor

The benefit of hybridisation is maximum for SM=1 hence, this condition (with no thermal storage) has been discussed. The annual energy to the grid can be partially attributed to solar and partially to hybridisation whenever hybridisation is used. The energy to the grid is proportional to the design capacity. So, a plot of these energies per MW is shown in Figure 27 while varying the hybridisation factor (and employing no thermal storage).

As can be noted, this plot is made for the condition of SM=1 and no thermal storage. Hence as hybridisation is increased, the solar field area does not increase. The electrical energy that is apportioned to solar increases as f_{hb} increases. This indicates that hybridisation is beneficial when there is no thermal storage.

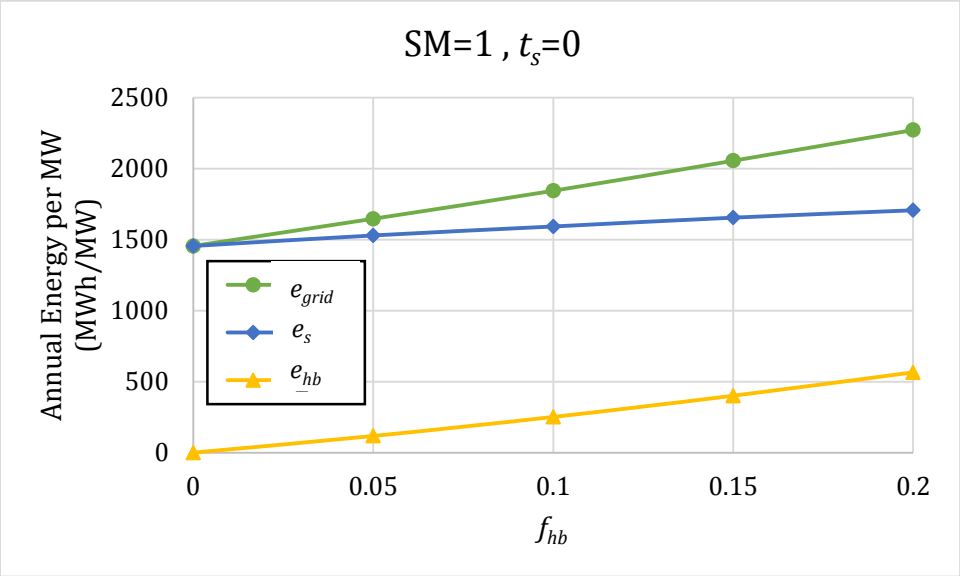

Figure 27: Variation of Annual Energy per MW with Hybridisation (t_s=0)

6.3.3. Effect of Hybridisation on Annual Efficiency Attributed to Solar Field

Figure 28 shows the variation of the annual solar to electric efficiency with SM for f_{hb}=0, 0.1 and 0.2 for 1 MW and 50 MW capacities (with no thermal storage). It can be seen that higher the hybridisation factor, higher is the overall efficiency. However, the benefit of hybridisation decreases as SM increases.

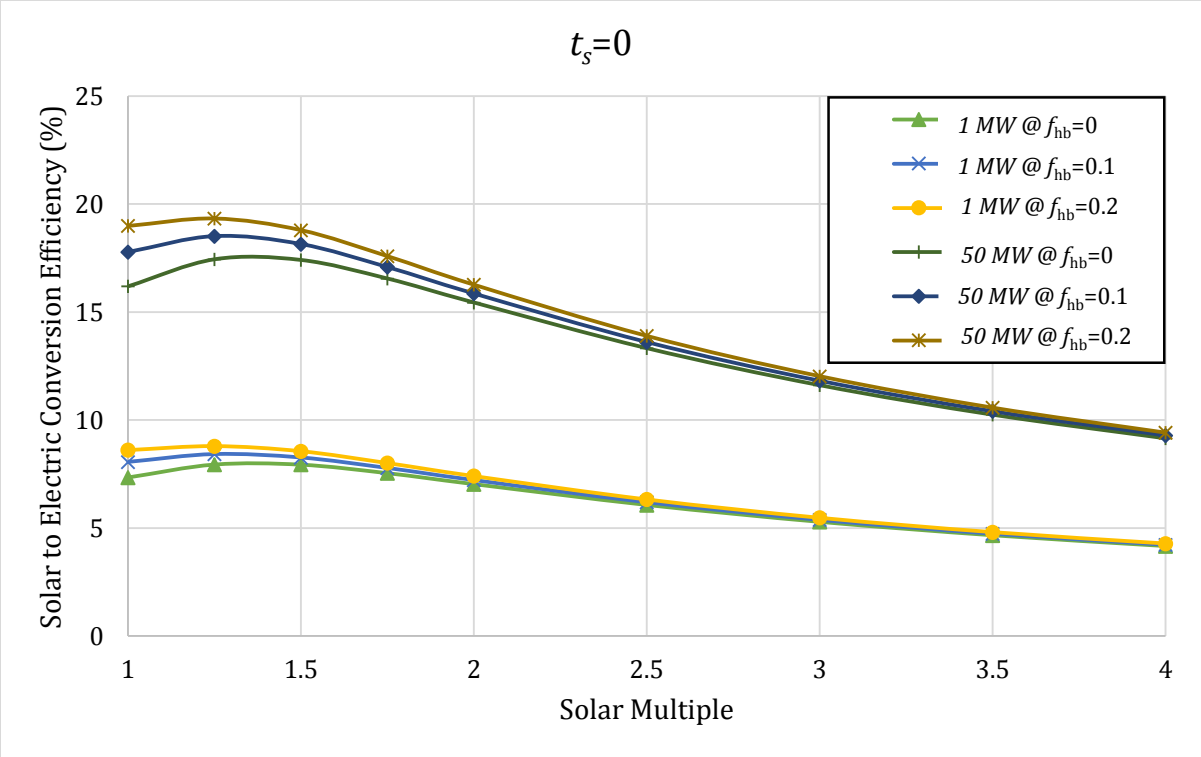

Figure 28: Variation of Annual Efficiency with SM for f_{hb} =0, 0.1 and 0.2 (t_s=0)

6.4. Thermal Storage and Hybridisation

The CUF is independent of the rated capacity of the plant. Figure 29 to Figure 31 show the variation of CUF with SM for zero, six and fifteen hours of storage respectively. In every figure, hybridisation values of 0, 0.1 and 0.2 are considered. It is seen that the CUF increases with SM but the benefit of hybridisation is maximum for SM=1 and decreases as SM increases as seen in the previous section.

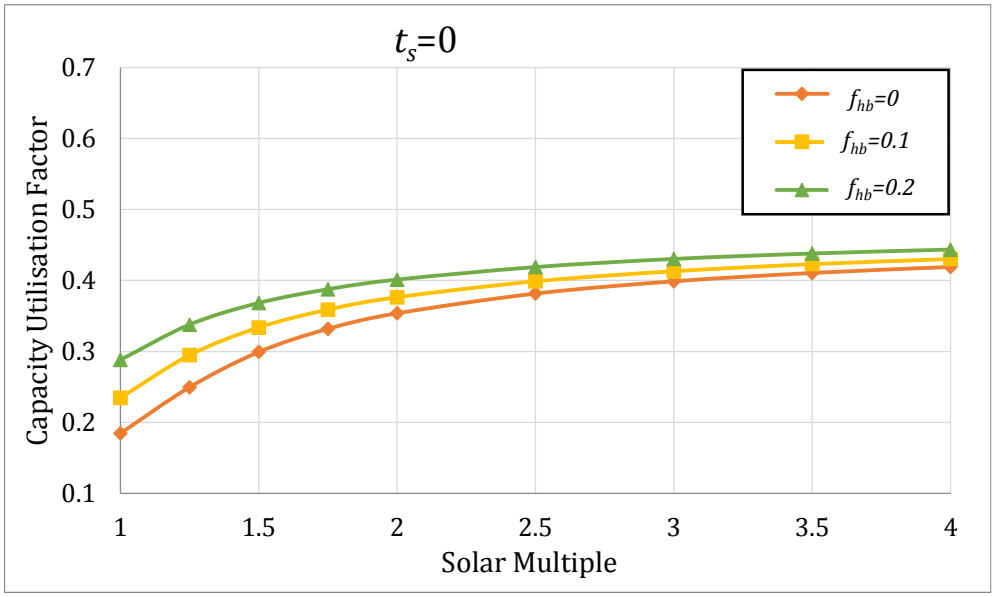

Figure 29: Variation of CUF with SM for t_s=0 hours and f_{hb} =0, 0.1 and 0.2

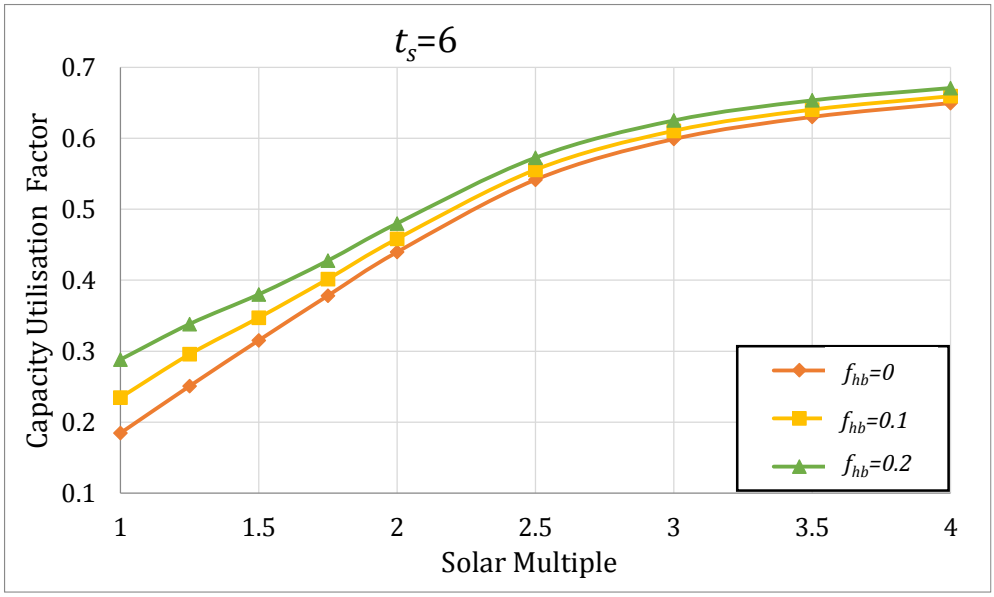

Figure 30: Variation of CUF with SM for t_s=6 hours and f_{hb} =0, 0.1 and 0.2

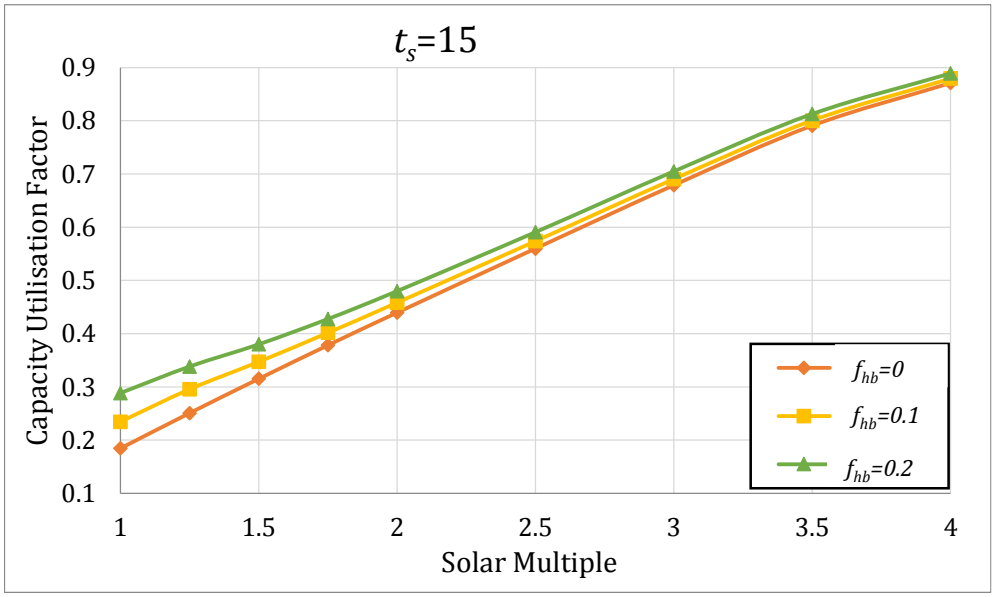

Figure 31: Variation of CUF with SM for t_s=15 hours and f_{hb} =0, 0.1 and 0.2

6.5. Height of Tower at Optimum SM (f_{hb}=0)

The height of the tower is a function of the capacity of the plant and the number of thermal storage hours employed.

Table 8 gives the heights of the tower for various capacities for thermal storage hours of 0, 6 and 15 hours (and no hybridisation) at their respective optimum SM. Note that the optimum SM does not vary with capacity for a given number of thermal storage hours. This case was taken just to give an idea of the variation of the tower heights with capacity at optimum SM.

Table 8: Tower Height for Various Plant Capacities at Optimum SM (f_{hb} =0)

Capacity (MW)	Height (m)		
	t_s = 0 SM=1.4	t_s = 6 SM=2.1	t_s = 15 SM=3.2
1	26	32	39
5	51	63	77
10	66	81	100
20	85	104	129
35	106	130	161
50	122	150	185

Figure 32 is a plot of the height vs. the capacity of the plant at the optimum SM values (and no hybridisation).

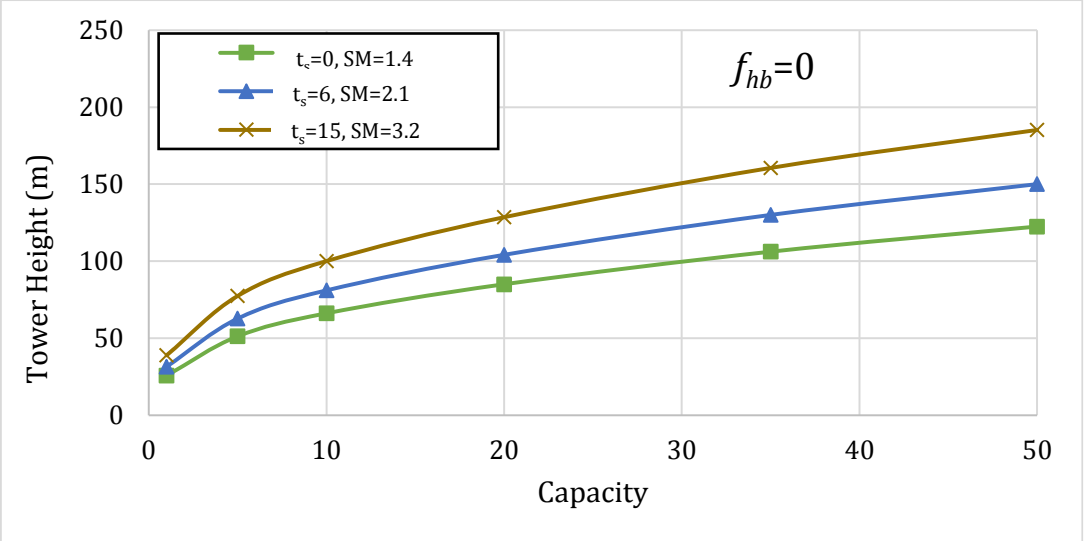

Figure 32: Tower Height vs. Capacity for t_s=0, 6 and 15 at Optimum SM (f_{hb} =0)

6.6. Comparison of Results for Clear vs. Hazy Day Attenuation Models

Attenuation, as explained earlier, depends upon the slant height of a heliostat from the top of the receiver. For a plant configuration, it depends only on the number of points chosen (boundary of plant) and their location.

The effect of attenuation for a case with six hours of storage, no hybridisation and SM=2.1 (optimum) is shown in Table 9.

Table 9: Effect of Attenuation for SM=2.1 (optimum) and t_s=6 hours (f_{hb}=0)

Capacity (MW)	Clear Day		Hazy Day	
	Annual Electrical Energy Generated (MWh)	η_{s-e} (%)	Annual Electrical Energy Generated (MWh)	η_{s-e} (%)
1	4059	8.77	4029	8.55
50	200343	19.11	193666	17.13

This case has been taken just as an example to illustrate the degree by which the annual electrical energy generated and solar to electric efficiency reduces when the hazy day model (<23 km visibility) is used. It is seen that the reduction is quite substantial when the capacity is high, the annual electrical energy reduces by 3.3% while η_{s-e} reduces by 10.4% (for a 50 MW plant). This is expected because for large capacities the field is bigger and hence the slant heights are consequently higher. The effects of haziness of the atmosphere are negligible for plants with smaller capacities.

Therefore, in actual practice, for analysing higher capacity plants, the hourly variation of atmospheric effects needs to be taken into consideration.

7. Conclusions and Future Work

In this report, a novel methodology has been provided to design a solar tower plant for a surround field configuration. Given, the location of the plant and corresponding DNI data, the capacity of the plant, number of thermal energy storage hours, maximum fraction of hybridisation permitted and efficiencies of various components associated with an ST plant, the objective of the methodology is to arrive at the optimum solar field, which would give the maximum annual solar to electric conversion efficiency. The proposed methodology uses a non-dimensional approach, which is unique, and arrives at the optimum size based on the concept of Solar Multiple.

In principle, the present methodology can be extended to a cavity type of receiver also. In this case, the angle subtended by opening of the receiver would be critical in order to arrive at the optimum size of the solar field.

Further, the optimisation of the solar field needs to be performed with respect to the cost per unit energy generated considering all the financial metrics applicable. A financial model would be developed in order to perform this exercise. This work would be undertaken subsequent to availability of the cost parameters of all the major components, since there is limited number of plants developed in Indian context. The detailed techno-economic analysis is likely to provide insights towards identifying research priorities and also developing a roadmap for cost reduction strategies for large scale adoption of Solar Tower technologies.

The methodology was developed for Solar Tower with Steam, for validation purposes. The tool designed & developed can be modularised in a manner that it can aid the sCO_2 based power systems also. This tool can be used by researchers for any pre-feasibility analysis of tower systems using sCO_2.

References

MA Ramaswamy, V. C. (2012). *Engineering Economic Policy Assessment of Concentrating Solar Technologies for India.* CSTEP.

MA Ramaswamy, T. N. (2014). *Global Review of Solar Tower Technology.* CSTEP.

ITP. (2012). *Realising the potential of concentrating Solar Power in Australia.* IT Power.

Stine B William, G. M. (2001). *Power From the Sun.*

Wikimapia. (n.d.). Retrieved 2015, from http://wikimapia.org/#lang=en&lat=37.445153&lon=-6.255856&z=16&m=b

Wikimapia. (n.d.). Retrieved September 2015, from http://wikimapia.org/#lang=en&lat=37.564548&lon=-5.326610&z=15&m=b

Srilakshmi, G., Venkatesh, V., Badri, R. S., Thirumalai, N., & Ramaswamy, M. (2014). *Global Review of Solar Tower Technology.* Bangalore: CSTEP.

(n.d.). (NREL) Retrieved 2016, from National Renewable Energy Laboratory: http://www.nrel.gov/csp/solarpaces/power_tower.cfm

Appendix 1

Determination of Packing Density Variation

For a solar tower plant, the concept of PD is used to define and get an idea about how the heliostats are packed in the given land.

This is especially important in the case of a solar tower plant because the mirrors are all placed such that shadowing and blocking effects of adjacent heliostats are minimised. Consequently, PD varies with location in the solar field. The definition of local PD is given by Equation 32.

$$Local\ Packing\ Density = \left(\frac{Mirror\ Area}{Land\ Area}\right)_{local} \quad (32)$$

In other words, it indicates the extent of utilisation of mirrors as a fraction of the local land area.

The local PD in general is a function of r/h for all existing plants having a radial staggered pattern.

The solar power received per unit area of the land depends on PD. The average overall PD for different plants can be calculated with the information available in the present literature (National Renewable Energy Laboratory, n.d.). But, the variation of PD with respect to r/h is not given.

The variation of PD with r/h based on a theoretical layout of a solar field (Stine B William, 2001) was examined. In addition to this the fields of three existing solar tower plants – Gemasolar (Wikimapia, n.d.), PS 10 and PS 20 (Wikimapia, n.d.) were studied and replicated in excel.

Field Replication

The Gemasolar plant in Spain shown in Figure 33a is an existing operational solar tower plant using an external cylindrical receiver and surround field. This field has 2650 heliostats with a larger north side.

On closer examination, it is noted that there are 38 circular rows. The first 27 rows form complete circles around the tower. However, the next 10 rows do not form complete circles around the tower. They stop at varying distances with the major part in the north side of the field.

Using Wikimapia, the radial distance of each row was measured. Additionally, the total number of heliostats was counted in each row. Consequently, the non-dimensionalised coordinates of each heliostat's centre position in the field were obtained. For the last 10 rows, the circumferential angles subtended by the end heliostats were measured and the heliostat positions were determined.

The same exercise was also performed for the other two plants, namely, PS 10 and PS 20 (see Figure 34a and Figure 35a). These two plants also have a radial staggered heliostat layout. However, they use cavity receivers and hence only have a single side (north) field.

Based on this exercise, the replicated fields (along with their originals) are shown in Figure 33 to Figure 35. It can be seen that the replicated field shows a very close comparison with the original images. This ascertains that the degree of error in the approximate measured radial distances is negligible.

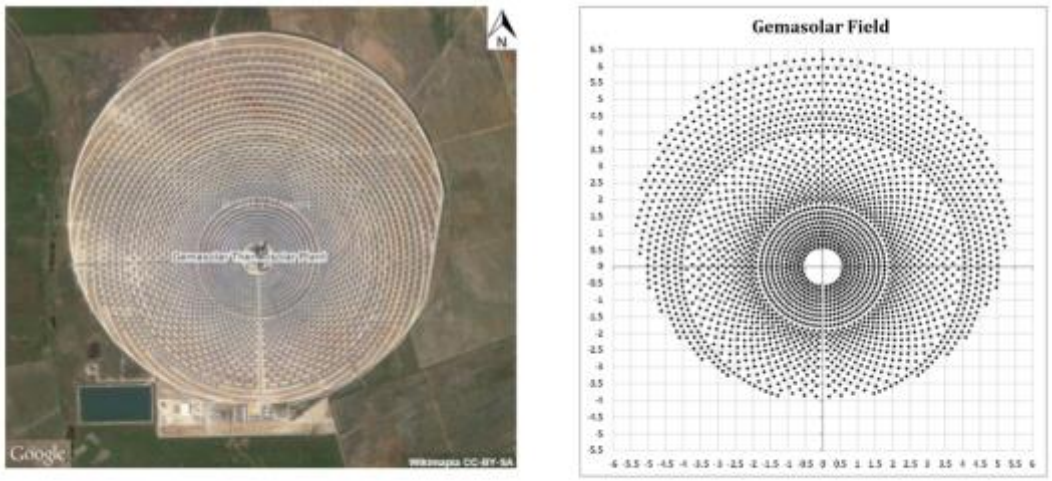

a) From Wikimapia b) Replication

Figure 33: Replication of Gemasolar Field in Excel (comparison)

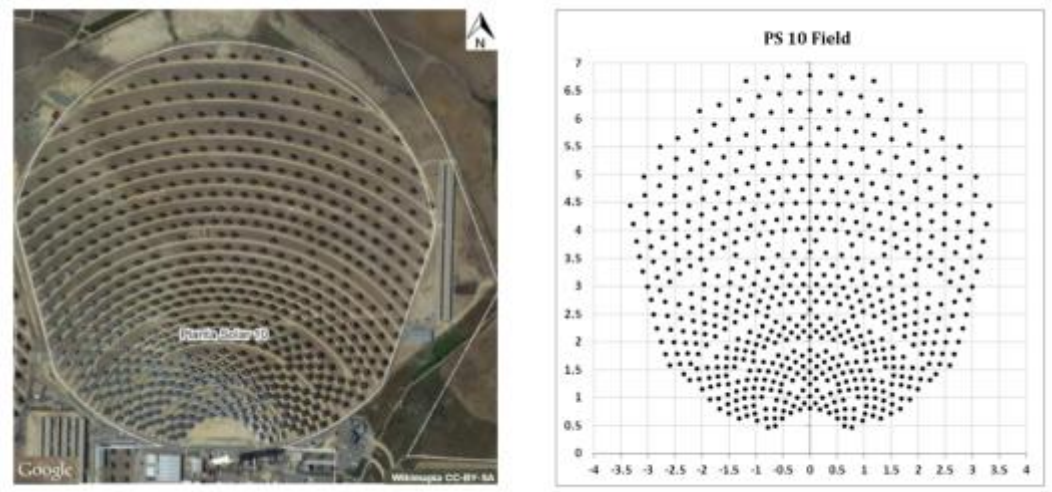

a) From Wikimapia b) Replication

Figure 34: Replication of PS 10 Field in Excel (comparison)

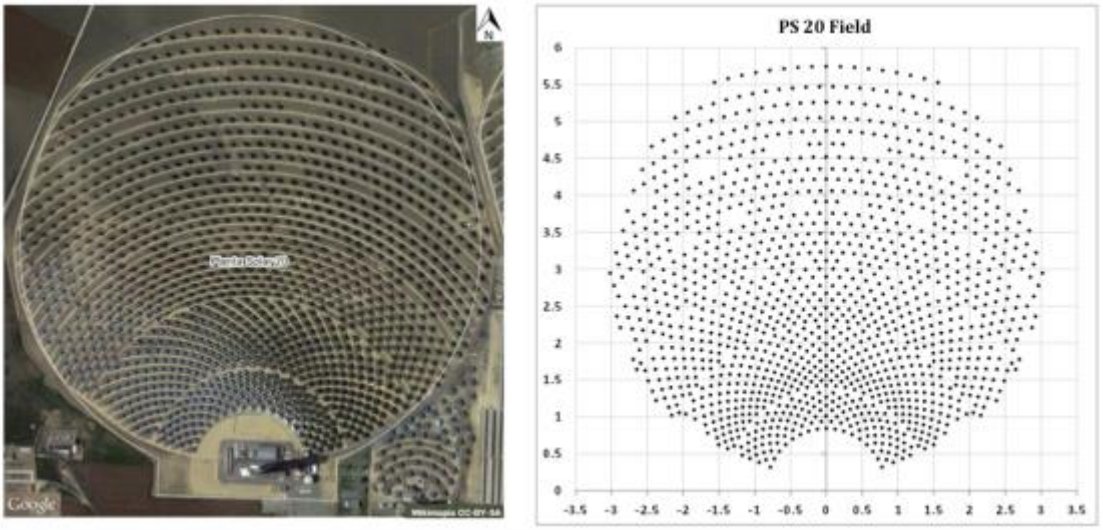

a) From Wikimapia b) Replication

Figure 35: Replication of PS 20 Field in Excel (comparison)

Gemasolar Plant

In order to look at the variation of PD with radial distance from the base of the tower, the PD of each row of heliostats was computed. The radial distance of each row (r) was measured. The first 27 rows are full circles. The last 10 rows (row 28 to 38) do not form complete circles. The angle subtended by the farthest two heliostats of each row plus half the circumferential angle between heliostats on each side was measured ($\Delta\theta$ in radians). This is shown in Figure 36.

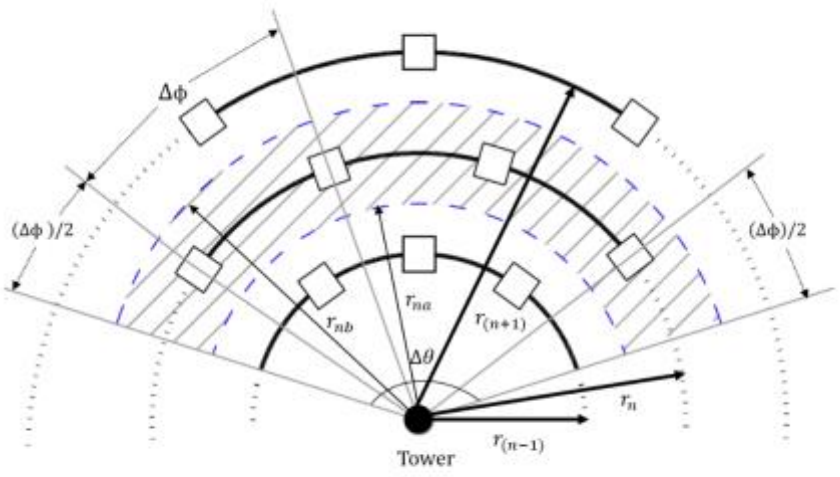

Figure 36: Local Packing Density Determination

As an example, in order to find out the PD of the n^{th} row, with radial distance r_n from the base of the tower, the following steps were followed (refer Figure 36).

1) Mirror area of this row (MA_n) is calculated using Equation 33.

$$MA_n = n_n \times A_{heliostat} \quad (33)$$

where n_n is the number of heliostats in the n^{th} row and $A_{heliostat}$ is the area of each heliostat (which is constant).

2) Land area of this row (LA_n) is taken as the area of the shaded region between the dotted circles (between the midpoints of the given row (n) with its adjacent rows) as can be seen in Figure 36. Radial distance of the previous row, $r_{(n-1)}$ and that of the next row, $r_{(n+1)}$ are considered.

3) The respective radial distances r_{na} , r_{nb} and land area of this row (LA_n) are calculated using Equation 34 and Equation 35.

$$r_{na} = \frac{r_{(n-1)} - r_{(n+1)}}{2} \text{ and } r_{nb} = \frac{r_{(n-1)} + r_{(n+1)}}{2} \quad (34)$$

$$LA_n = \{\Delta\theta(r_{nb}^2 - r_{na}^2)\}/2 \quad (35)$$

PD_n, the PD of the n^{th} row is calculated using Equation 36.

$$PD_n = \frac{MA_n}{LA_n} \quad (36)$$

In this way, PD for each row was computed. It may be noted that when the row is a complete circle, $\Delta\theta = 2\pi, (360°)$.

PS 10 and PS 20 Plants

For these plants, PD was calculated as was done for the last 10 rows of the Gemasolar plant (the subtended angle was measured and the corresponding land area was calculated for that row).

Determination of Nominal Variation of *Packing Density* with *r/h*

Figure 37 shows the PD variation for the existing plants and the theoretical variation that was given in (Stine B William, 2001). It may be seen, that this theoretical value is not in conformity with the existing practical data (Figure 37). Therefore, to obtain a nominal PD variation with r/h, data of the existing plants was used. It can be seen that from this data, at around $\frac{r}{h} = 2$ and $\frac{r}{h} = 4$, jumps occur (Figure 37). This happens because in the staggered pattern, the circumferential distance between heliostats increases as r increases and at $\sim\frac{r}{h} = 2$ and 4, these distances become large enough to introduce additional heliostats between them. The radial gaps are also increased to avoid blockage effects. So, the local mirror area suddenly increases (for the next row) and the jump in PD occurs. However, for defining the nominal PD variation, PD jumps have been avoided and curve fits of the data were obtained as given as follows (Equation 37 to Equation 39):

$$PD = 0 \quad \text{for } \frac{r}{h} < \left(\frac{r}{h}\right)_{min} \quad (37)$$

$$PD = 0.492 - 0.0939\frac{r}{h} \quad \text{for } \left(\frac{r}{h}\right)_{min} \leq \frac{r}{h} \leq 2.8 \tag{38}$$

$$PD = \frac{0.6}{\sqrt{\left(\frac{r}{h}\right)^2 - 1}} \quad \text{for } \frac{r}{h} > 2.8 \tag{39}$$

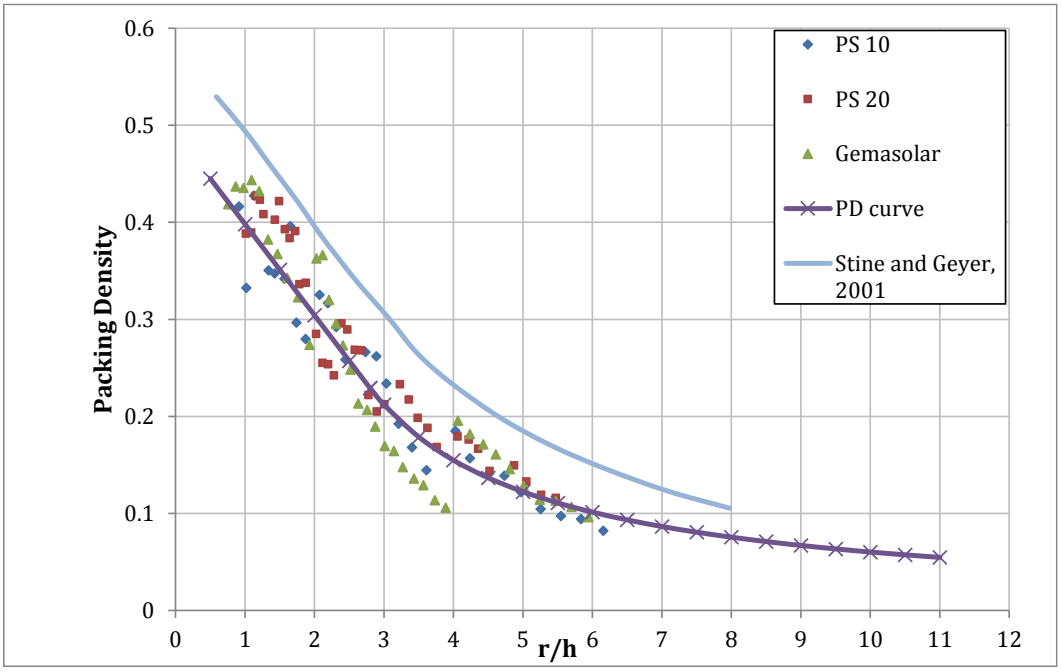

Figure 37: Curve Fits Chosen to Account for Packing Density

It may be noted that PD is mainly a function of r/h and not dependent on the azimuth angle.

The equations mentioned above are used while taking into account variation of the PD of heliostats in determination of the contours of annual solar energy per unit land area.

Appendix 2

Comparison of Solar Field Boundary with Contours of e_l to Enable Choice of Boundary

It was proposed (in Section 3.4), that taking PD into consideration and generating the contours of constant solar energy per unit land area is better suited for fixing the field boundary. The reason for this is depicted in Figure 38 to Figure 41 which show that contours of e_l somewhat closely correspond to the field boundaries of existing plants as compared to e_m which shows no resemblance to existing field boundaries. Here, the heliostat fields of Gemasolar, Crescent Dunes PS 10 and PS 20 plants have been compared.

From the Figures, one can say that the appropriate equi-energy contour compare reasonably well quantitatively, with the actual boundaries used in existing plants. Gemasolar and PS 20 field boundaries seem to match with a contour value (in MWh/m^2) of 0.18, Crescent Dunes with 0.145 and PS 10 with 0.155.

Based on this observation, a possible seed value for the energy value per unit land area as the nominal boundary value can be that corresponding to an e_l value of ~0.16 ($\pm$0.02), for the general preliminary design for solar tower plants. In the detailed design one can conduct a sensitivity analysis on this number and choose the optimum value based on iterations.

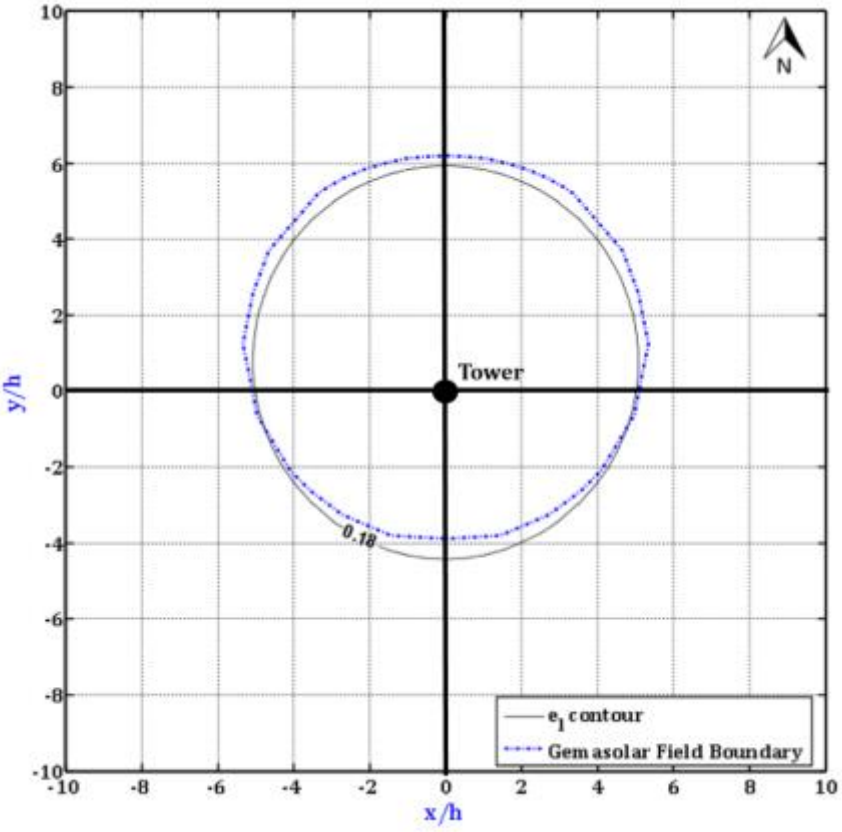

Figure 38: Gemasolar Field Boundary and el field contour at Seville

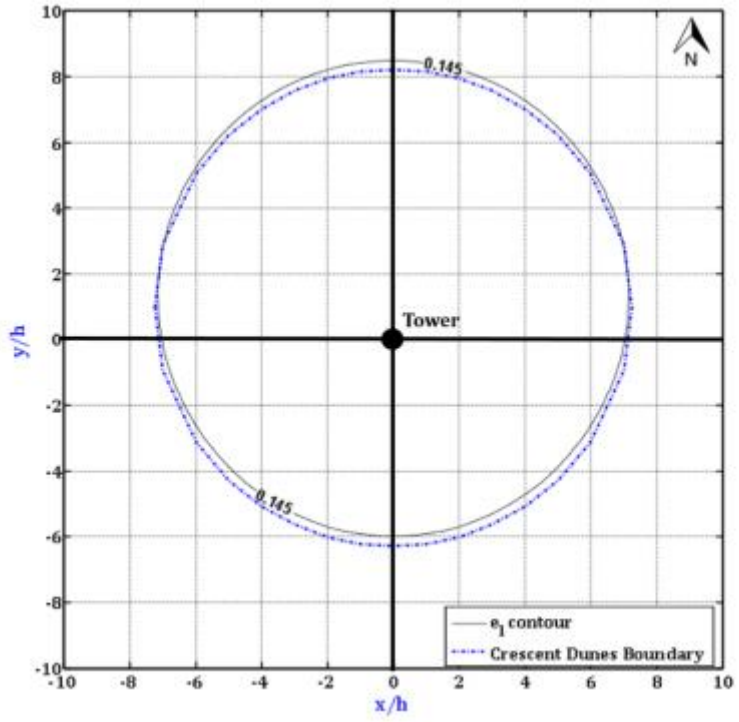

Figure 39: Crescent Dunes Field Boundary and el field contour at Tonopah

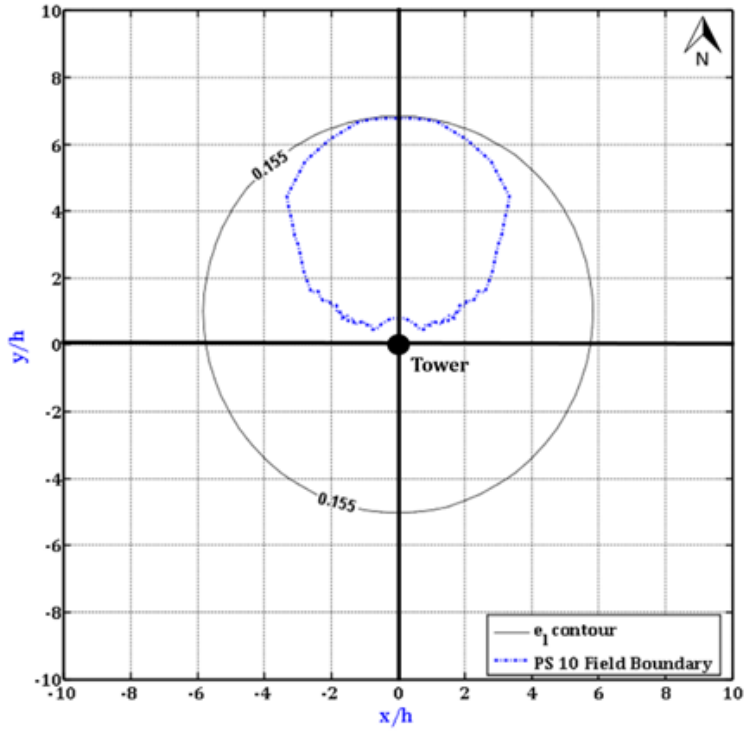

Figure 40: PS 10 Field Boundary and el field contour at Seville

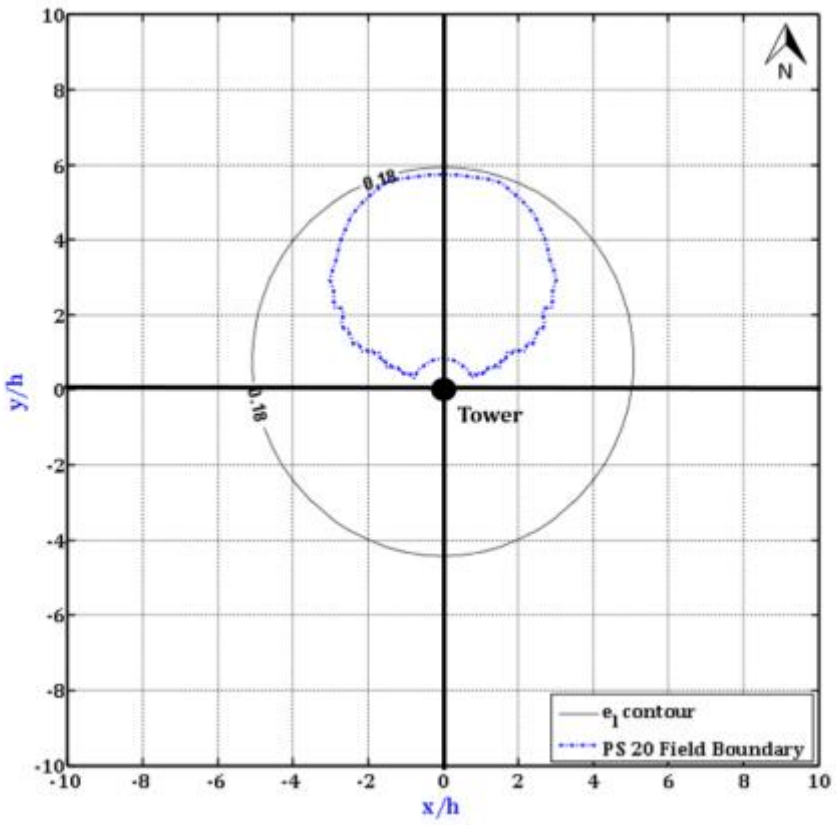

Figure 41: PS 20 Field Boundary and e_l field contour at Seville

Appendix 3

Flowchart of the Methodology (used for coding)

Inputs and Calculation of Design Parameters

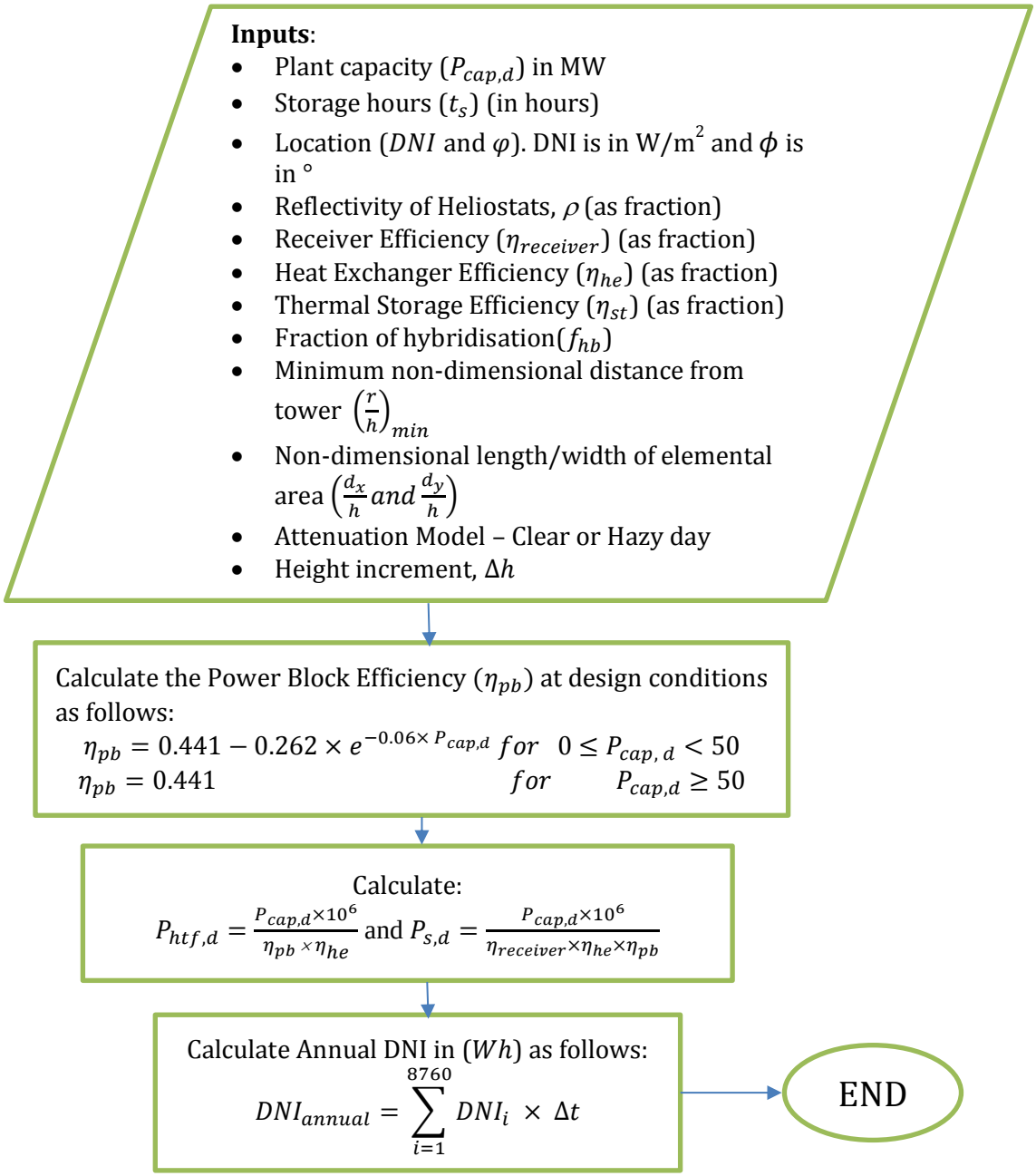

Fixing the Field Boundary

Vary x/h and y/h values from $(-10,-10)\ to (10,10)$ in steps of $\frac{d_x}{h}$ and $\frac{d_y}{h}$ by sweeping y/h for each step of x/h where h is the height of the tower

↓

Calculate annual reflected energy per unit land area, e_l ,(discrete area around each point)

↓

For each position of the heliostat $(x/h,\ y/h)$ and latitude (φ)

↓

Calculate

$$\frac{r}{h} = \sqrt{\left(\frac{x}{h}\right)^2 + \left(\frac{y}{h}\right)^2}$$

↓

Calculate Packing Density of point (PD) as follows:

$PD = 0$ for $\frac{r}{h} < \left(\frac{r}{h}\right)_{min}$;

$PD = 0.492 - 0.0939\frac{r}{h}$ for $\left(\frac{r}{h}\right)_{min} \leq \frac{r}{h} \leq 2.8$;

$PD = \frac{0.6}{\sqrt{\left(\frac{r}{h}\right)^2 - 1}}$ for $\frac{r}{h} > 2.8$

↓

Calculate the following for each hour ($i = 1\ to\ 8760$) and store in an array
All angles are in degrees

a) $Declination,\ Del,\ \delta$: $\delta = 23.45 \times sin\left\{\left(\frac{360}{365}\right) \times (284 + n)\right\},\ n\ varies\ from\ 1\ to\ 365$

b) $Hour\ Angle,\ \omega$: $\omega = 15 \times (t - 0.5 - 12),\ t\ varies\ from\ 0\ to\ 24$

c) $Zenith\ Angle,\ \theta_Z$: $\theta_Z = \cos^{-1}\{(\cos\phi\cos\delta\cos\omega) + (\sin\phi\sin\delta)\}$

d) $Altitude\ angle,\ alpha, \alpha$: $\alpha = 90 - \theta_Z$

e) $Azimuth\ angle,\ A$: $A^1 = \cos^{-1}\left[\frac{\sin\delta\cos\phi - \cos\delta\sin\phi\cos\omega}{\cos\alpha}\right]\ if\ \sin(\omega) > 0,\ A = 360 - A^1,\ else\ A = A^1$

↓

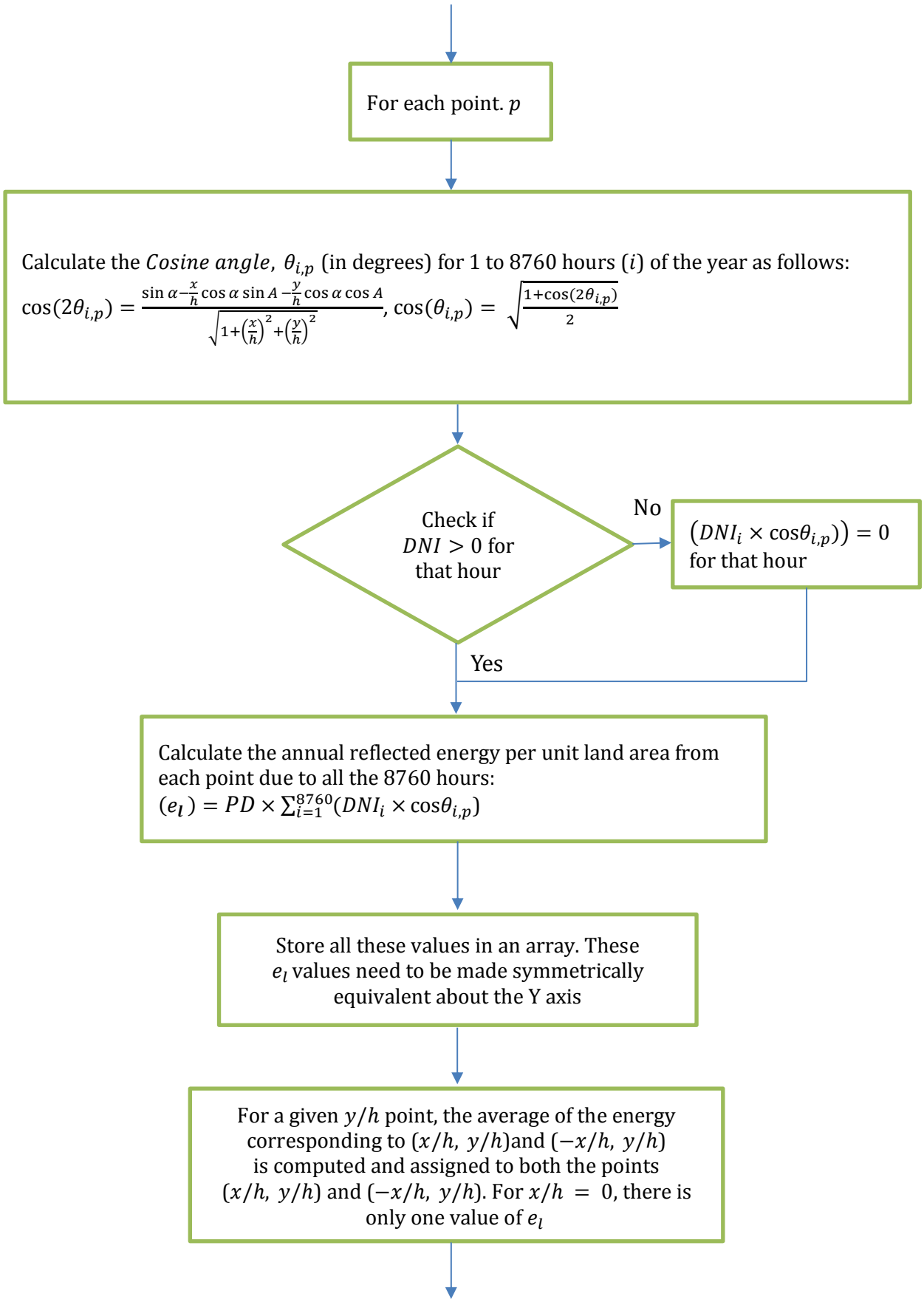
For each point. p
Calculate the $Cosine\ angle,\ \theta_{i,p}$ (in degrees) for 1 to 8760 hours (i) of the year as follows:
$\cos(2\theta_{i,p}) = \frac{\sin\alpha - \frac{x}{h}\cos\alpha\sin A - \frac{y}{h}\cos\alpha\cos A}{\sqrt{1+\left(\frac{x}{h}\right)^2+\left(\frac{y}{h}\right)^2}}$, $\cos(\theta_{i,p}) = \sqrt{\frac{1+\cos(2\theta_{i,p})}{2}}$
Check if $DNI > 0$ for that hour
No
$(DNI_i \times \cos\theta_{i,p})) = 0$ for that hour
Yes
Calculate the annual reflected energy per unit land area from each point due to all the 8760 hours:
$(e_l) = PD \times \sum_{i=1}^{8760}(DNI_i \times \cos\theta_{i,p})$
Store all these values in an array. These e_l values need to be made symmetrically equivalent about the Y axis
For a given y/h point, the average of the energy corresponding to $(x/h,\ y/h)$and $(-x/h,\ y/h)$ is computed and assigned to both the points $(x/h,\ y/h)$ and $(-x/h,\ y/h)$. For $x/h\ =\ 0$, there is only one value of e_l

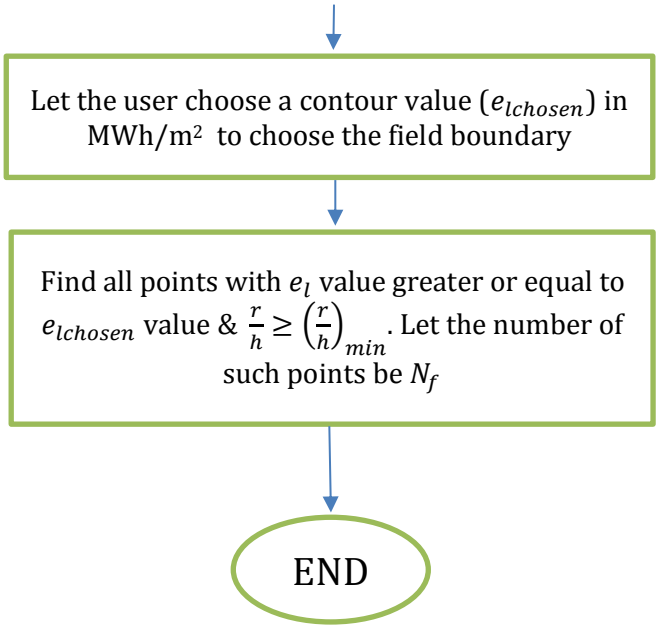
Let the user choose a contour value ($e_{lchosen}$) in MWh/m² to choose the field boundary
Find all points with e_l value greater or equal to $e_{lchosen}$ value & $\frac{r}{h} \geq \left(\frac{r}{h}\right)_{min}$. Let the number of such points be N_f
END

Determination of Tower Height as SM=1

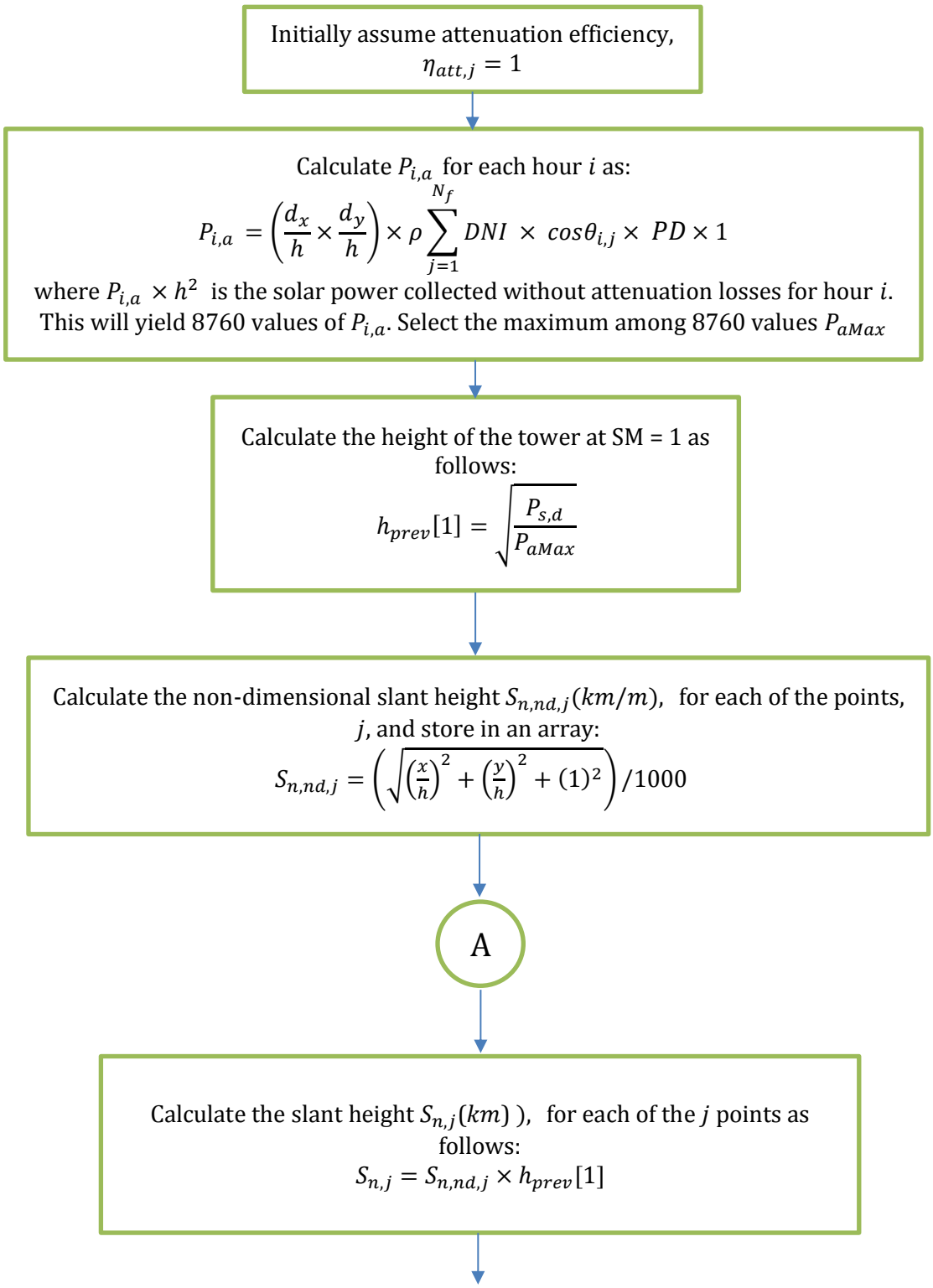

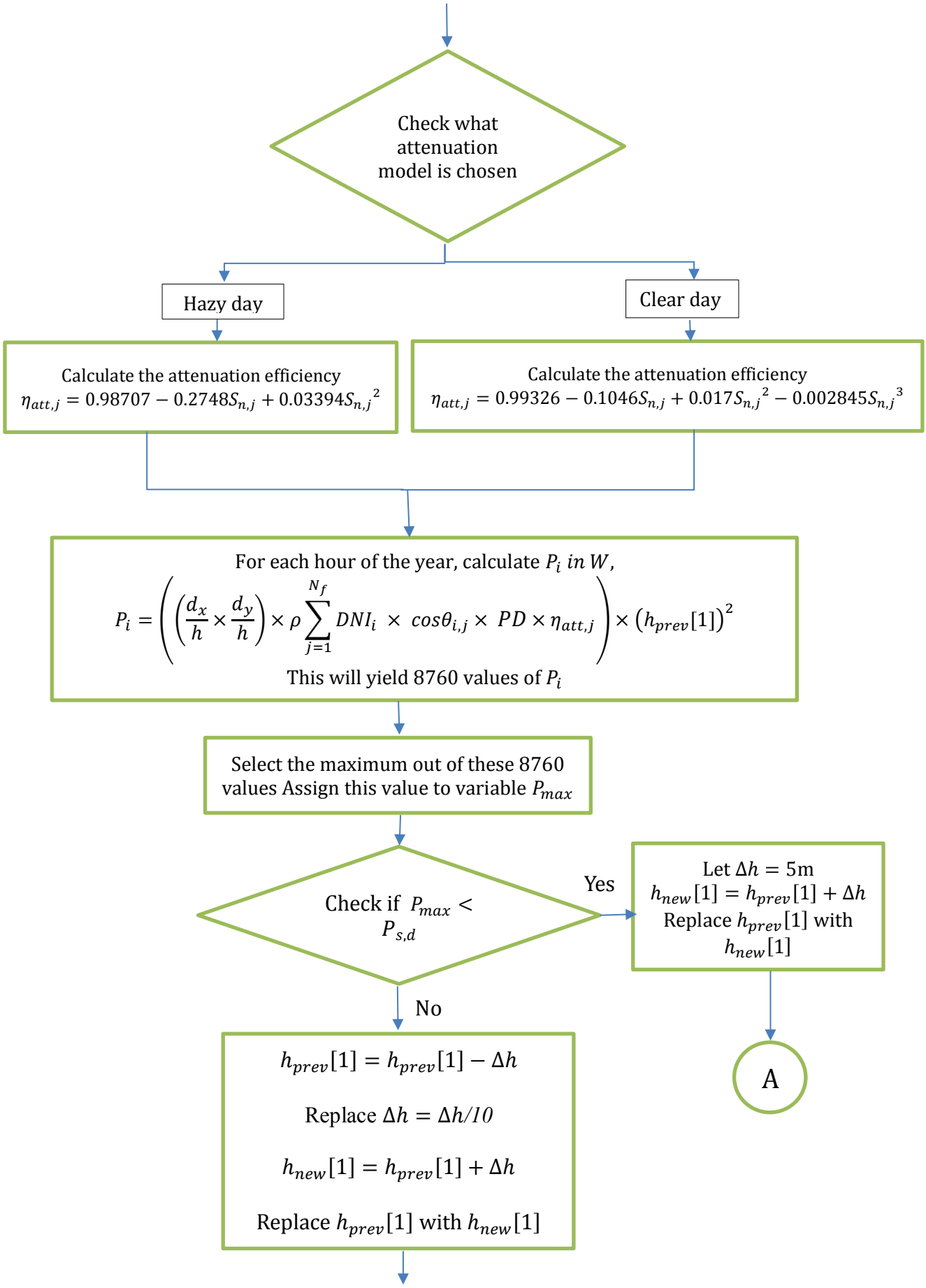
Check what attenuation model is chosen
Hazy day
Clear day
Calculate the attenuation efficiency $\eta_{att,j} = 0.98707 - 0.2748S_{n,j} + 0.03394{S_{n,j}}^2$
Calculate the attenuation efficiency $\eta_{att,j} = 0.99326 - 0.1046S_{n,j} + 0.017{S_{n,j}}^2 - 0.002845{S_{n,j}}^3$
For each hour of the year, calculate P_i in W,
$P_i = \left(\left(\frac{d_x}{h} \times \frac{d_y}{h}\right) \times \rho \sum_{j=1}^{N_f} DNI_i \times cos\theta_{i,j} \times PD \times \eta_{att,j}\right) \times \left(h_{prev}[1]\right)^2$
This will yield 8760 values of P_i
Select the maximum out of these 8760 values Assign this value to variable P_{max}
Check if $P_{max} < P_{s,d}$
Yes
Let $\Delta h = 5$m
$h_{new}[1] = h_{prev}[1] + \Delta h$
Replace $h_{prev}[1]$ with $h_{new}[1]$
A
No
$h_{prev}[1] = h_{prev}[1] - \Delta h$
Replace $\Delta h = \Delta h/10$
$h_{new}[1] = h_{prev}[1] + \Delta h$
Replace $h_{prev}[1]$ with $h_{new}[1]$

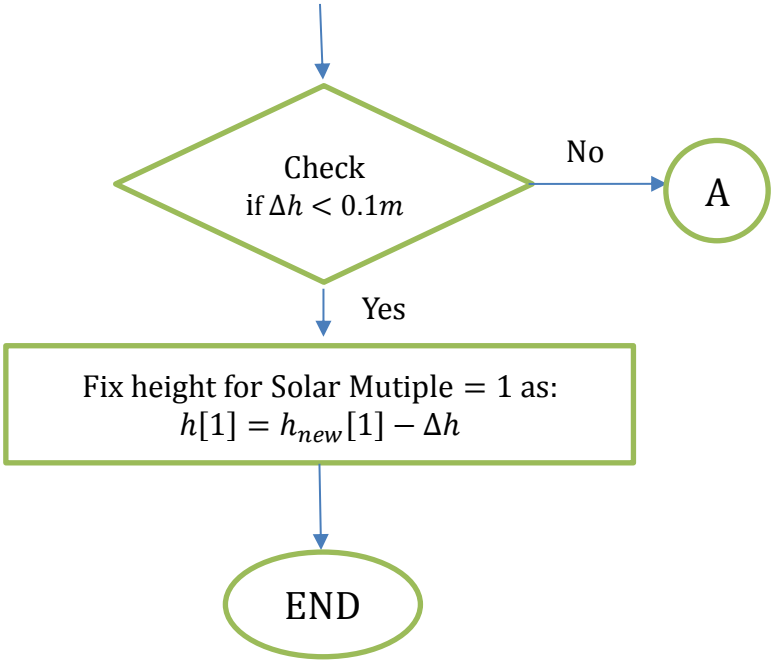
Check
if $\Delta h < 0.1m$
No
A
Yes
Fix height for Solar Mutiple = 1 as:
$h[1] = h_{new}[1] - \Delta h$
END

Estimation of Hourly Energy from Field and Energy Computations

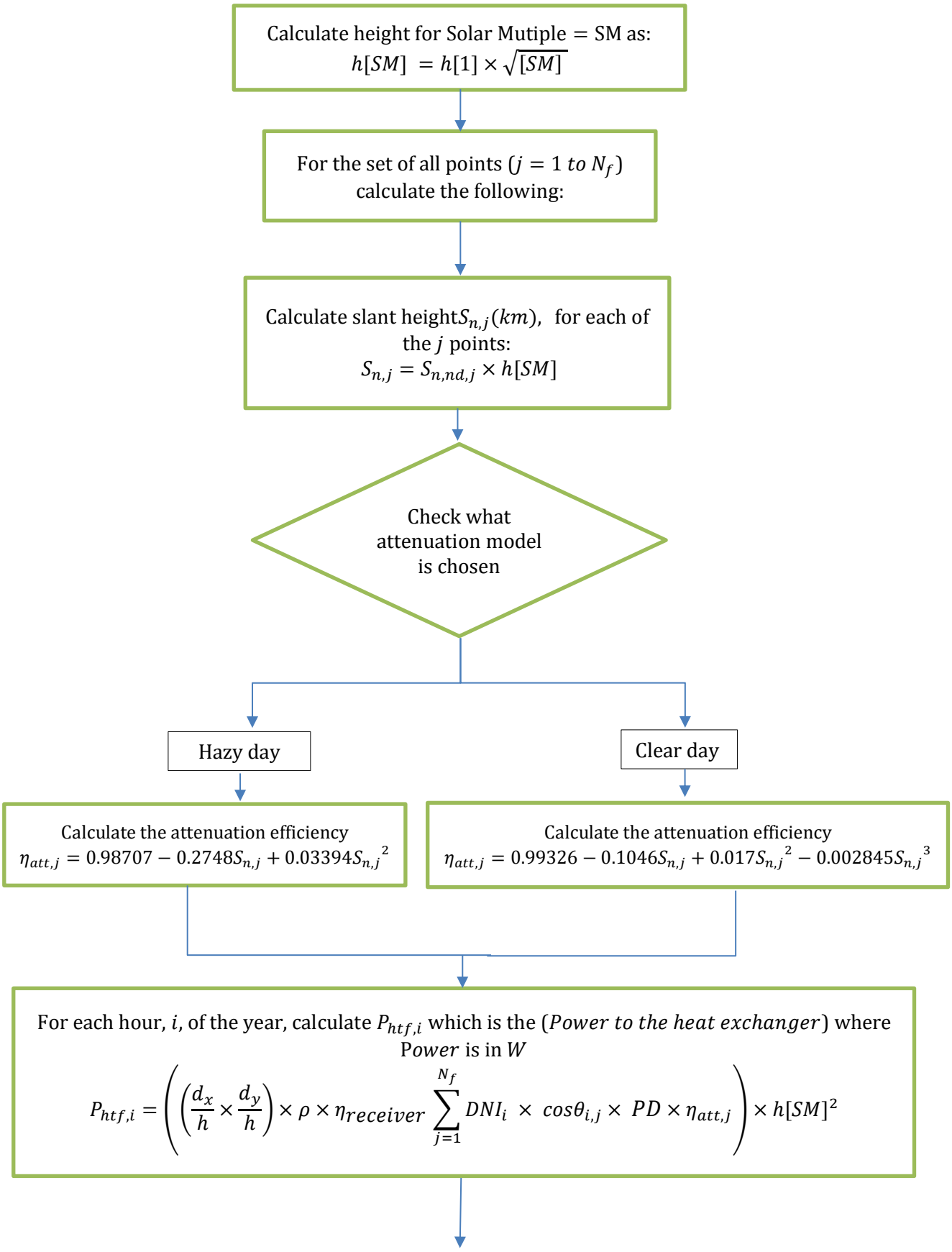

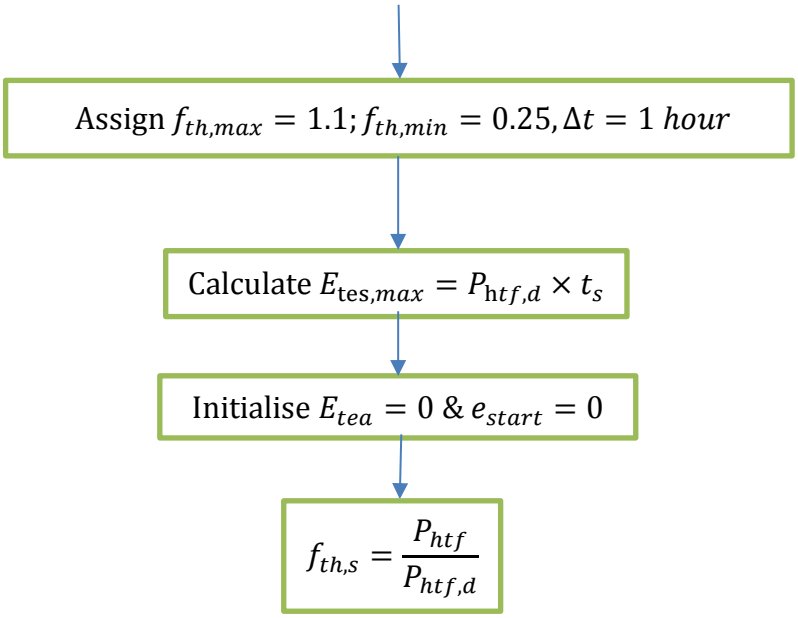
Assign $f_{th,max} = 1.1; f_{th,min} = 0.25, \Delta t = 1\ hour$
Calculate $E_{\text{tes},max} = P_{\text{htf},d} \times t_s$
Initialise $E_{tea} = 0$ & $e_{start} = 0$
$f_{th,s} = \frac{P_{htf}}{P_{htf,d}}$

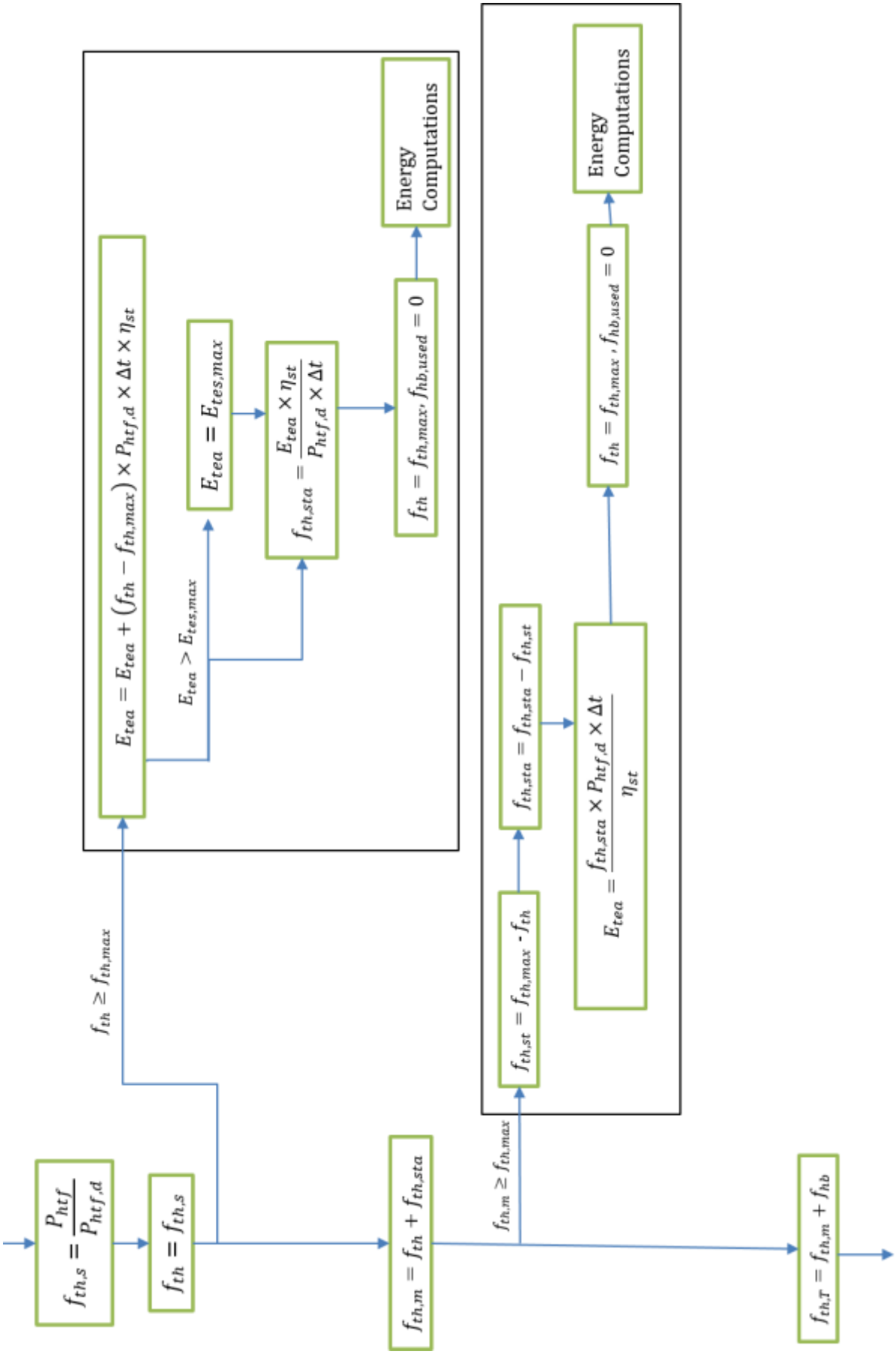
$f_{th,s} = \frac{P_{htf}}{P_{htf,d}}$
$f_{th} = f_{th,s}$
$f_{th} \geq f_{th,max}$
$E_{tea} = E_{tea} + (f_{th} - f_{th,max}) \times P_{htf,d} \times \Delta t \times \eta_{st}$
$E_{tea} > E_{tes,max}$
$E_{tea} = E_{tes,max}$
$f_{th,sta} = \frac{E_{tea} \times \eta_{st}}{P_{htf,d} \times \Delta t}$
$f_{th} = f_{th,max}, f_{hb,used} = 0$
Energy Computations
$f_{th,m} = f_{th} + f_{th,sta}$
$f_{th,m} \geq f_{th,max}$
$f_{th,st} = f_{th,max} - f_{th}$
$f_{th,sta} = f_{th,sta} - f_{th,st}$
$E_{tea} = \frac{f_{th,sta} \times P_{htf,d} \times \Delta t}{\eta_{st}}$
$f_{th} = f_{th,max}, f_{hb,used} = 0$
Energy Computations
$f_{th,T} = f_{th,m} + f_{hb}$

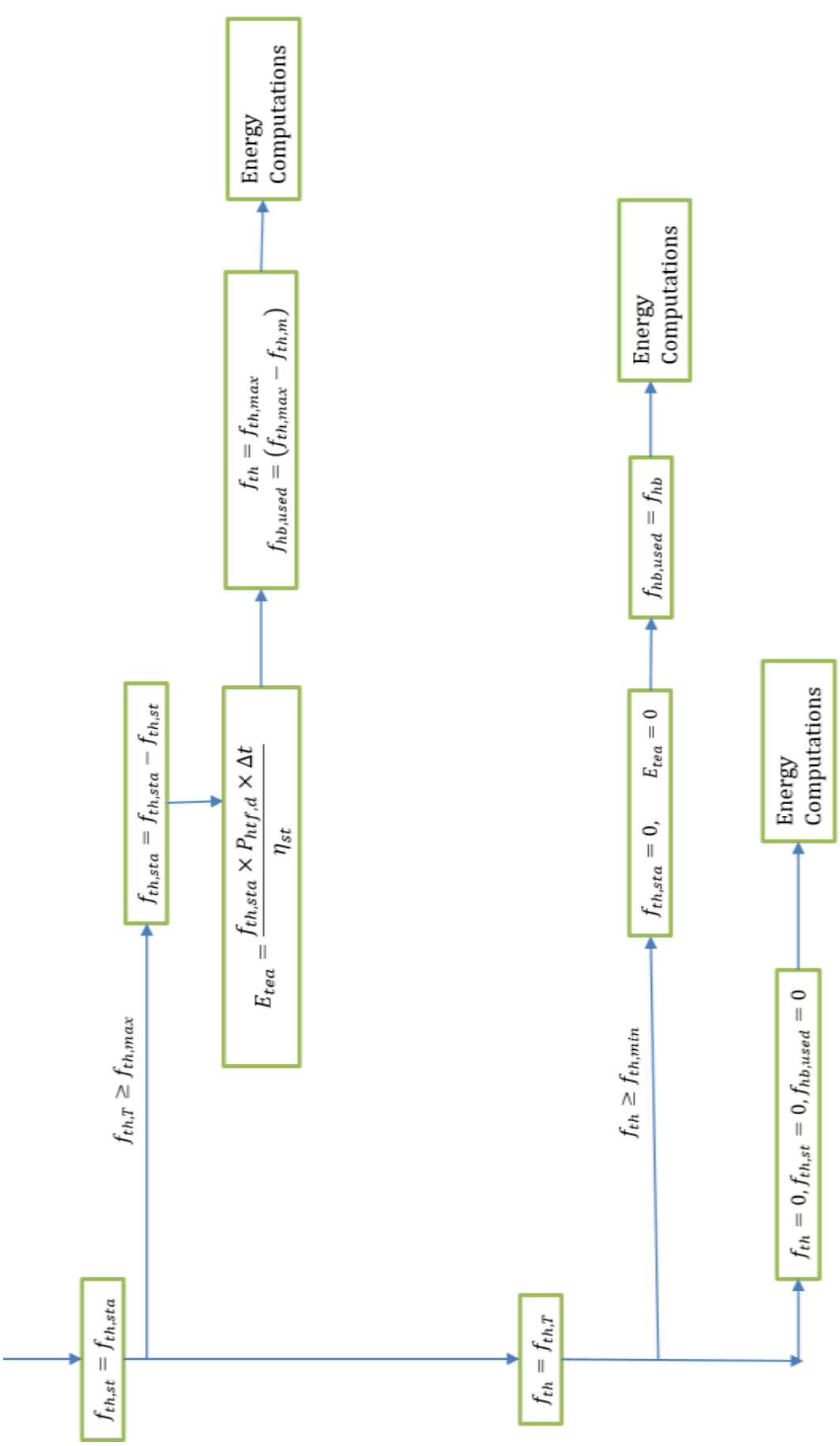
$f_{th,st} = f_{th,sta}$
$f_{th,T} \geq f_{th,max}$
$f_{th,sta} = f_{th,sta} - f_{th,st}$
$E_{tea} = \frac{f_{th,sta} \times P_{htf,d} \times \Delta t}{\eta_{st}}$
$f_{th} = f_{th,max}$
$f_{hb,used} = (f_{th,max} - f_{th,m})$
Energy Computations
$f_{th} = f_{th,T}$
$f_{th} \geq f_{th,min}$
$f_{th,sta} = 0, \quad E_{tea} = 0$
$f_{hb,used} = f_{hb}$
Energy Computations
$f_{th} = 0, f_{th,st} = 0, f_{hb,used} = 0$
Energy Computations

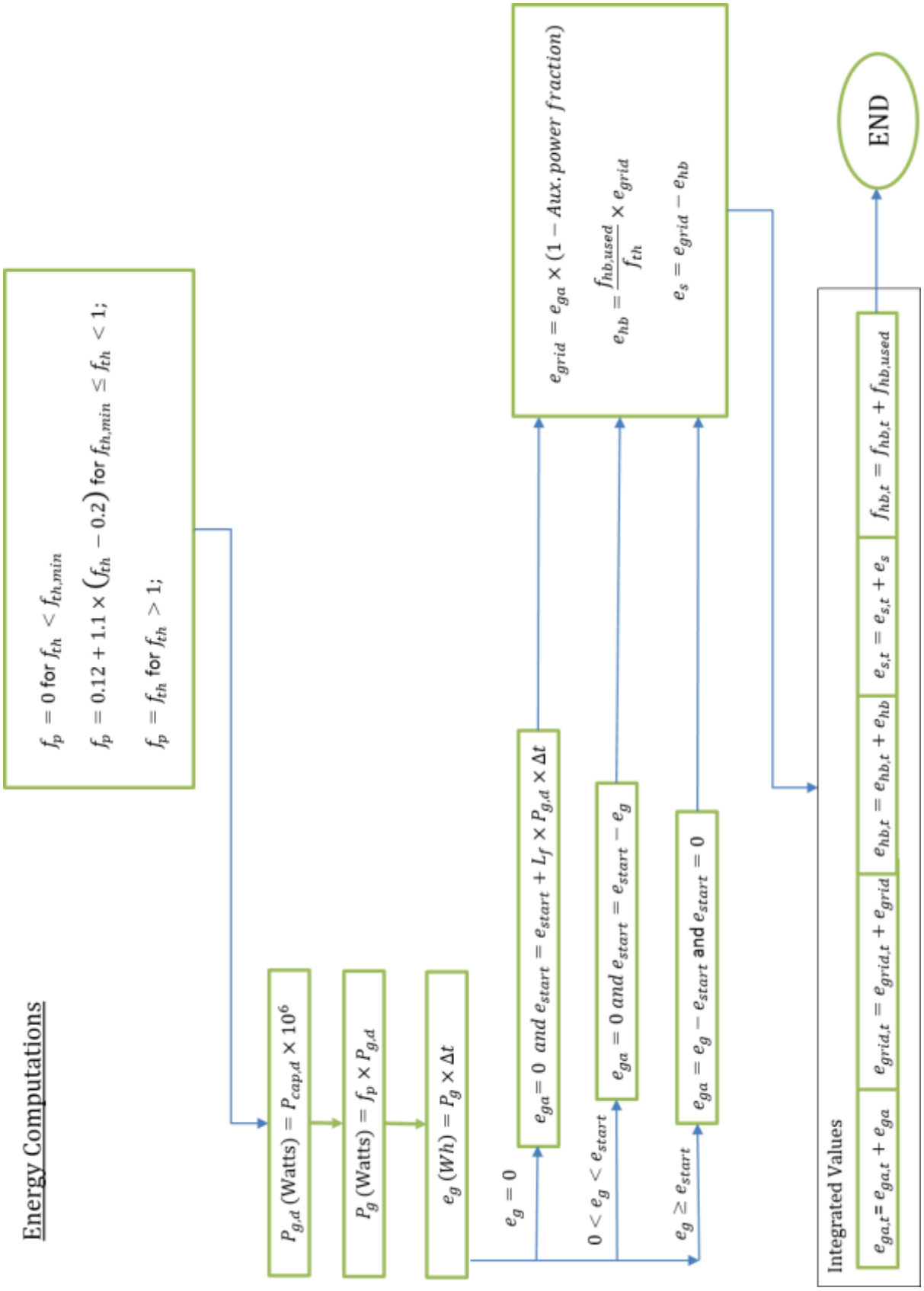
Energy Computations
$f_p = 0$ for $f_{th} < f_{th,min}$
$f_p = 0.12 + 1.1 \times (f_{th} - 0.2)$ for $f_{th,min} \leq f_{th} < 1$;
$f_p = f_{th}$ for $f_{th} > 1$;
$P_{g,d}$ (Watts) $= P_{cap,d} \times 10^6$
P_g (Watts) $= f_p \times P_{g,d}$
e_g (Wh) $= P_g \times \Delta t$
$e_g = 0$
$e_{ga} = 0$ and $e_{start} = e_{start} + L_f \times P_{g,d} \times \Delta t$
$0 < e_g < e_{start}$
$e_{ga} = 0$ and $e_{start} = e_{start} - e_g$
$e_g \geq e_{start}$
$e_{ga} = e_g - e_{start}$ and $e_{start} = 0$
$e_{grid} = e_{ga} \times (1 - Aux.power\ fraction)$
$e_{hb} = \frac{f_{hb,used}}{f_{th}} \times e_{grid}$
$e_s = e_{grid} - e_{hb}$
Integrated Values
$e_{ga,t} = e_{ga,t} + e_{ga}$
$e_{grid,t} = e_{grid,t} + e_{grid}$
$e_{hb,t} = e_{hb,t} + e_{hb}$
$e_{s,t} = e_{s,t} + e_s$
$f_{hb,t} = f_{hb,t} + f_{hb,used}$
END

Calculation of Land Area, Mirror Area, CUF and η_{s-e}

Calculate Land Area (LA) as follows:

$$LA = \left\{\left(N_f \times \left[\frac{d_x}{h} \times \frac{d_y}{h}\right]\right) + \left(\pi \times \left(\left(\frac{r}{h}\right)_{min}\right)^2\right)\right\} \times (h[SM])^2$$

Calculate Mirror Area (MA) as follows:

$$MA = \left(\sum_{j=1}^{N_f} PD\right) \times \left(\frac{d_x}{h} \times \frac{d_y}{h}\right) \times (h[SM])^2$$

Calculate the Capacity Utilisation Factor as follows:

$$\text{CUF} = \frac{e_{ga,t}}{P_{g,d} \times 8760}$$

Calculate the Solar to Electric Conversion Efficiency as follows:

$$\eta_{s-e} = \frac{e_{s,t}}{MA \times (Annual\ DNI)}$$

END

Center for Study of Science, Technology and Policy

#18, 10th Cross, Mayura Street, Papanna layout

Nagashettyhalli, RMV II Stage, Bengaluru-560094

Karnataka, India

www.cstep.in